2008

Theoretical modeling of cortisol sensor

Milorad Gordic
University of South Florida

Theoretical Modeling of Cortisol Sensor

By

Milorad Gordic

A thesis submitted in partial fulfillment
of the requirements for the degree of
Master of Science in Biomedical Engineering
Department of Chemical and Biomedical Engineering
College of Engineering
University of South Florida

Major Professor: Shekhar Bhansali, Ph.D.
Alberto Sagues, Ph.D.
Vinay Gupta, Ph.D.
Arun Kumar, Ph.D.
Shyam Aravamudhan, Ph.D.

Date of Approval:
October 27, 2008

Keywords: Dielectrophoresis, Square Wave Voltammetry, BioMEMS, Electrochemistry,

Thiol Chemistry

DEDICATION

To all students who are currently pursuing their education while being a full-time employee… There were countless moments when I thought of quitting while working on this thesis, but somehow found a reason not to… To my entire family who supported me and always encouraged me, never to give up… To all who prayed for me every night for enlightenment and patience to finish this thesis (especially my wife Daniella, my mother Anica, my sister Ruzica, and my now deceased grandmother Pera and nanny Manda)… And to all whom I may be forgetting... Thank you from the bottom of my heart! This dissertation is dedicated to all of you.

ACKNOWLEDGEMENTS

I would like to extend special thanks to Dr. Shekhar Bhansali and Dr. Arun Kumar for inviting me to be a part of the Cortisol Sensor project. I also wish to thank Dr. Alberto Sagues for his help and guidance with electrochemistry. Thanks to Dr. Shyam Aravamudhan, Dr. Niranjan Ramgir, Ke, Dorielle and Brian for assisting me in fabrication and analysis of the sensor itself. I would like to extend thanks to all of the committee members for their input to the project. And last but not least, thank you, Lord, for all your blessings.

TABLE OF CONTENTS

LIST OF TABLES

LIST OF FIGURES

Theoretical Modeling of Cortisol Sensor

Milorad Gordic

ABSTRACT

This thesis describes the theoretical modeling of a response of an electrochemical BioMEMS sensor for detecting small amounts of cortisol hormone. The electrochemical sensor utilizes a catalyst enzyme (3α-HSD) to convert cortisone to cortisol and the Square Wave Voltammetry (SWV) as a preferred method to measure the forward and reverse current of the system. The parameters and equations necessary to estimate the Square Wave Voltammetry (SWV) theoretical response are determined and outlined. The response is modeled and the results are compared to the experimental data. Further, the design of the sensor is analyzed and suggestions are made on how to improve the repeatability of the sensor's response.

The diffusion coefficients for cortisone and cortisol hormone are calculated to be $2.87*10^{-10}$ and $2.84*10^{-10}$ m^2/s respectively with ± 10% tolerance. The dimensionless peak current (ψ) for the system is ~10% lower than the one theoretically postulated by Bard et al. [3]. The surface area of the working electrode of the sensor varies with and is directly proportional to the concentration of the analyte. Theoretical current peaks are hypothesized to be within 10% tolerance limits (mainly due to the reason that the surface area of the working electrode is itself a variable).

CHAPTER 1

HISTORY OF CORTISOL RESEARCH

Just like many other hormones, corticosteroids (a family of steroid hormones produced by the adrenal gland) were discovered through their absence from a system. In 1849 British scientist Thomas Addison observed a fatal form of anemia, as he described it at the time, which was reflected by diseased supra-renal capsules (glands located above the kidneys). In a later description of the condition, which came to be known as Addison's disease, he emphasized the weakness of the body and the heart, anemia, irritability of the stomach, and discoloration of the skin. However, it was not until 70 years later that the distinction between the adrenal hormones was first seen through the administration of the extracted substance from the adrenal gland that extended life. The functions of these substances were further divided into those that involve carbohydrate metabolism (glucocorticoids), and those related to electrolyte and water balance (mineralocorticoids). However, it was found that with the administration of these substances, certain side effects occurred which reflected themselves by causing patients to gain weight, develop "moon face" and "buffalo hump" (from the excess fat-tissue stored in these areas), osteoporosis of the spine, insulin resistant diabetes, etc. More than 80 years after Addison's disease was named (primarily characterized by insufficient secretion of adrenal gland), Cushing's disease was described (primarily characterized by

an over-active adrenal gland and excess amounts of glucocorticoids). These conditions further motivated research into glucocorticoids. Then in 1949, Hench, Kendall, Slocumb, and Polley published a paper that turned out to be a major scientific breakthrough of its time. In it, they discussed the anti-inflammatory effects of the adrenal glucocorticoid hormone. The discovery benefited millions of people; however, dangerous side effects were still present since the effect of the new drugs did not include those of mineralocorticoids [10]. The above-mentioned scientists are considered to be the discoverers of the cortisol hormone, as we know it today. Ever since its discovery in 1949, cortisol has been thoroughly researched by scientists worldwide. Extensive research has been done to understand multiple roles cortisol has on a system [12, 19, 24, 32], but one can still say that its detection (using sensors) is in its infancy. This work is aimed at developing a cortisol sensor for medical and defensive purposes, and the following sections focus on its significance in both fields.

1.1 Introduction to Cortisol (Hydrocortisone)

Cortisol is a member of glucocorticoids – a family of steroid hormones produced by the adrenal gland. It has multiple roles and functions in the human system, including maintaining normal blood glucose levels, blood pressure regulation, and regulating the homeostatic balance of cardiovascular system, immune system, kidneys, skeletal muscle, nervous system, and endocrine system [10, 18].

It is not possible to make a quick estimate of how much cortisol is in an individual's bloodstream at a particular instance, partly due to the numerous factors affecting its levels. Levels of cortisol vary throughout the day, being highest in the

morning, and lowest right before bed-time, and after we fall asleep. Some controllable factors that can affect levels of cortisol are eating patterns and levels of activity throughout a day. Although, there are many changes in the system that can cause disruption of levels of cortisol hormone in the blood, none has been more effective than physical and/or emotional stress. As a matter of fact, stress is so effective in disrupting levels of cortisol that the hormone received a pet name – "stress-hormone".

Side effects of abnormal levels of cortisol range from case to case, and in some instances can even be beneficial. Most of the time, however, abnormal levels of cortisol are associated with negative side effects, often resulting in a serious condition after prolonged, untreated exposure. Addison's and Cushing's disease are, unfortunately, only two examples that can result in such an instance. Cortisol is thought to be a possible precursor to some other conditions such as epilepsy [9]. Developing a fast and reliable method of cortisol detection would be very beneficial; later in this chapter we will discuss the motivation behind the work described in this thesis.

1.2 Synthesis of Cortisol Hormone

Synthesis of most steroid hormones starts with cholesterol. Contrary to popular belief, cholesterol is essential for the homeostatic balance in the system. The organism produces most of it, but a good portion comes from food intake through daily consumption.

Since the adrenal gland has no visible innervation, it can be inferred that the Adrenocorticotropic hormone (ACTH) is a sole stimulant to production of cortisol. The adrenal gland does not store the cortisol hormone, but it does store significant amount of

its precursors. Once the ACTH stimulates the gland, cholesterol concentration drops within a very short time and the level of cortisol increases [18]. Although there is no documented research to support this, one could surmise that the relationship between adrenal cholesterol and cortisol is somewhat inversely proportional.

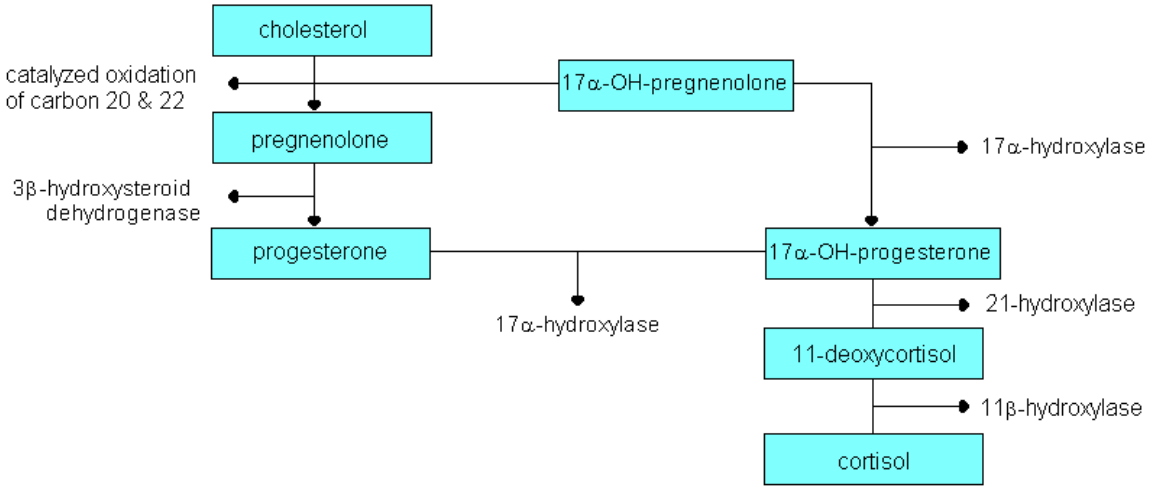

Figure 1.1: Synthesis of Cortisol

In order to fully understand the synthesis of cortisol, it is necessary to first understand that the entire process will undergo a few reactions involving enzymes critical for the creation of each hormone at a particular stage. First, the cholesterol will undergo a catalyzed oxidation of carbons 20 and 22. This reaction will result in pregnenolone and aldehyde, which then oxidizes into an isocaproic acid. In this reaction a small amount of 17α-OH-pregnenolone may also be formed; however, this portion will be converted to 17α-OH-progesterone by the 17α-hydroxylase enzyme. Although tiny portions of pregnenolone escape from the adrenal gland, most stays and undergoes further processing. The remaining pregnenolone is then converted to progesterone by 3β-hydroxysteroid dehydrogenase and involves two microsomal enzymes. Progesterone is

converted to 17α-OH-progesterone by the 17α-hydroxylase enzyme. Finally, this hormone goes through two more hydroxylation phases before it is finally converted to cortisol (see figure 1.1 and 1.2) [19].

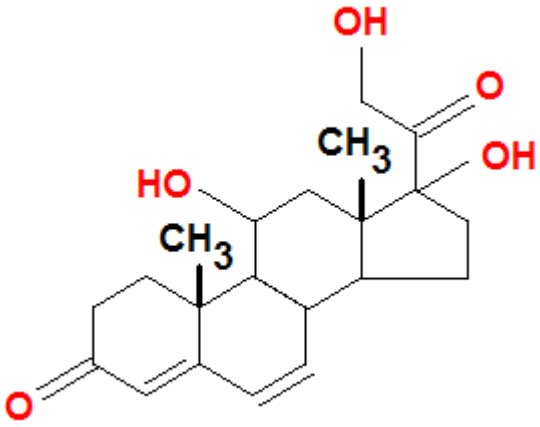

Figure 1.2: Structure of Cortisol ($C_{21}H_{30}O_5$).
Adapted from Citizendium. Online encyclopedia. 10/2008

Each enzyme from figure 1.1 is crucial for that particular step. Having an enzyme deficiency will not result in creation of cortisol, and exposure to such conditions over a prolonged period of time will result in a serious homeostatic imbalance.

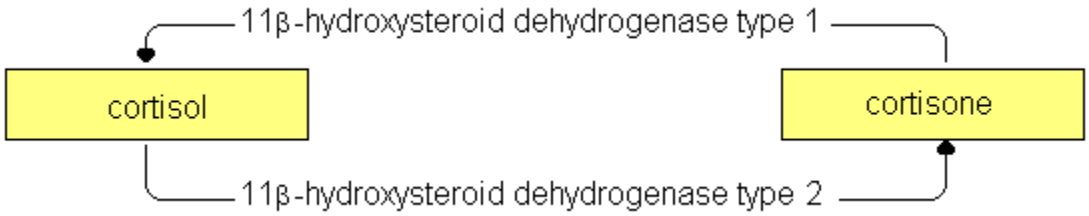

Figure 1.3: Cortisone ⇔ Cortisol Conversion

Further, inter-conversion between active cortisol to inactive cortisone and vice versa may be possible by introduction of another enzyme called 11β-hydroxysteroid dehydrogenase type 1 (11β-HSD-1) and 11β-hydroxysteroid dehydrogenase type 2 (11β-HSD-2) (see figure 1.3) [19].

1.3 Secretion of Cortisol Hormone

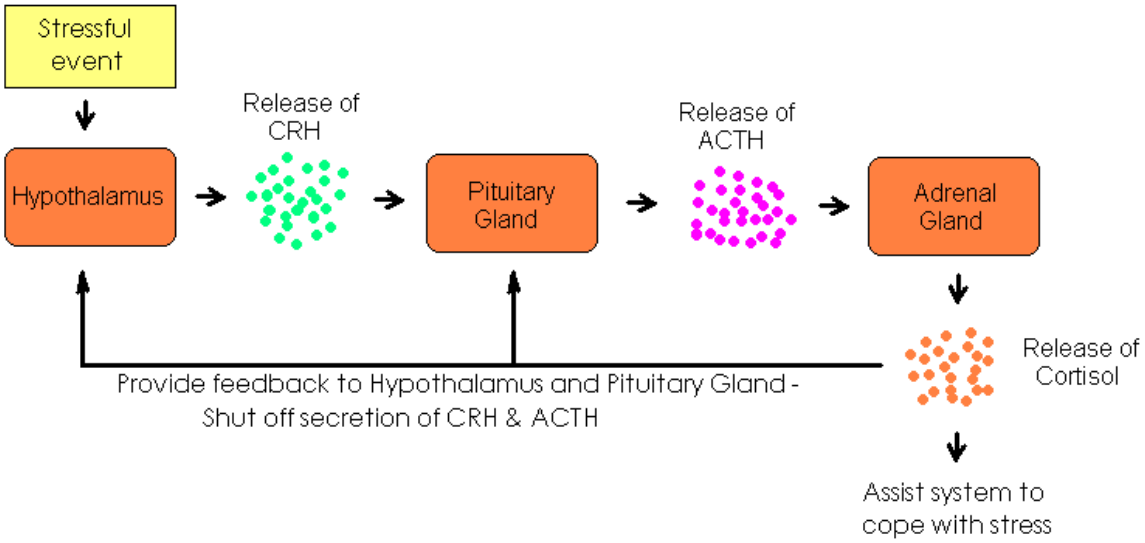

Figure 1.4: Secretion of Cortisol

The pathway to release of cortisol is relatively simple to explain. During a stressful event, for example, the hypothalamus starts releasing Corticotropin-releasing hormone (CRH). The Corticotropin-releasing hormone (CRH) triggers the release of Adrenocorticotropic hormone (ACTH) by the pituitary gland. Finally, it is the release of the Adrenocorticotropic hormone (ACTH) that stimulates the release of glucocorticoids (mainly cortisol) by the adrenal gland. Rising levels of cortisol will then provide feedback to the hypothalamus and pituitary gland and signal to stop the release of the Corticotropin-releasing hormone (CRH) and Adrenocorticotropic hormone (ACTH) (See figure 1.4) [18]. Transcortin, a protein serum, is responsible for transporting cortisol throughout the system [32]. As such, most cortisol hormones are bound to some kind of compound in the bloodstream. Only 4-10 % of the cortisol is thought to be free-moving in the system [12].

As mentioned earlier, levels of cortisol hormone will constantly vary throughout the day, being highest in the morning and lowest at night, right before the bed-time. In normal adults, providing they are not under stress, normal secretion of cortisol hormone in a whole day is 10-20mg. Morning levels vary anywhere between 140-180ng/ml, while afternoon and night levels significantly drop to anywhere between 20-40ng/ml [10]. The rate of increase/decrease of cortisol at any particular instance (i.e. epileptic seizure attack) is not known. This area of medicine is still open for further study and research.

1.4 Need for Cortisol Sensing

Detection of cortisol potentially has a wide variety of uses in the medical field, but these could also be applied to any other industry. A potential new market for a highly reliable cortisol sensor might be customs screening or airport screening for passengers carrying illicit materials (assuming that such passengers' stress levels would be unusually abnormal when compared to the norm). Another possible use for a highly sensitive cortisol sensor could be a form of polygraph screening to improve the accuracy of the test. The possibilities are endless.

1.4.1 Need for Cortisol Sensor in Medical Field

As mentioned, the cortisol sensor would have numerous applications in the medical field. Cortisol is one of the major metabolic regulators in the body, and as such, abnormal levels could indicate some other, more serious condition. Reliably detecting precise levels of cortisol might also give better idea about the level of cortisone in the system and its ratio to cortisol (two hormones that can be inter-converted using 11β-

hydroxysteroid dehydrogenase type 1 and 2 enzymes, as already shown). For example, children with hypoadrenalism have a lower range of cortisol as opposed to cortisone, while children with adrenal cancer have been found to have increased levels of cortisol as opposed to cortisone [21].

Another important recent discovery ties cortisol with an epileptic seizure attack [9]. Having a cortisol sensor would help further research into exactly what enables canines to predict an epileptic seizure. Since cortisol is a steroid and stress hormone, the possibility whether it is this hormone that dogs sense could further be researched. In other words, can canines smell an epileptic seizure as well as fear?

Also, the dangerous side effects of artificial cortisol used as a drug to treat certain conditions, such as, rheumatoid arthritis, cannot be forgotten. Overdosing a patient will most definitely result in Cushing's syndrome and later in Cushing's disease. Having a sensor to monitor the natural levels of cortisol, and then feeding back the automatic drug-delivery system could potentially minimize the negative side effects that such patients can experience.

Finally, another possible market for a reliable sensor is in the field of sports medicine. Well over the last forty years, athletes have been illegally using glucocorticoids to enhance their performance. Drug screening for illegal use of artificial steroids is yet another possible use of this kind of sensor [23].

1.4.2 Need for Cortisol Sensor in Other Fields

There are many possible industrial applications for a cortisol sensor, but none have the appeal like the possible screening tool for people importing illicit materials into

a country. While a terrorist threat is at an all time high and lives of innocent people are in danger all around the globe, having a sensor to monitor the stress level of passengers going through customs or airport security would be a great advantage. The heart rate, blood pressure, and other conditions connected to sympathetic nervous system, become abnormal in most people with any kind of confrontation [16]. Having a good cortisol monitor could segregate highly stressed travelers as opposed to ones experiencing low or no stress at all when confronted by customs agents.

Another application where a cortisol sensor might potentially find a use is the polygraph machine. Along with monitoring for respiratory rate, sweatiness of fingertips, blood pressure, and heart rate, the machine could monitor cortisol secretion and improve in accuracy. Also, biological research facilities that study the effect of man-made objects on flora and fauna mainly test the cortisol levels in the blood of a subject. For example, one particular study focused on the effect a fluctuating hydro-power plant had on one-year old trout [8]. The researchers in this study mainly focused on the level of blood cortisol and the nature of its secretion.

1.5 Collection of Sample

To monitor cortisol levels requires collecting two specimens of blood (collected between 6 and 8am and 6 to 11pm) or continuous collection of urine over a 24-hour period. For blood, two 5ml samples are collected and mixed with anticoagulant to keep the sample in liquid state. Upon receiving a sufficient amount of sample, the sample is then transferred in a refrigerated environment to the laboratory where it is analyzed using a preferred method.

1.6 Motivation

The basic motivation of this thesis is to investigate the possibility of an electrochemical sensor and its sensitivity to increasing levels of cortisol. While the most common methods for cortisol level diagnosis are still blood and urine tests, other potential methods for cortisol analysis are saliva and sweat tests.

Since cortisol levels in the human body differ throughout the day, blood and urine tests require repeatable sample collections throughout the day. Collecting all samples for analysis (especially blood) can result in a traumatic experience for the patient and it takes considerable time to implement – another down-side to the whole process. Having a highly selective sensor integrated within an instrument that could monitor either saliva and/or sweat throughout the day could not only reduce the trauma of the sample collection but also may aid in giving an insight into an epileptic seizure attack and serve as an aid to customs agents for separating passengers who may have malicious.

Clearly, there is a need for a cortisol sensor. There are also many ways to produce it, but finding an effective one is where the puzzle starts. In this thesis, the possibility of using the electrochemical sensing of the cortisol-biotin-streptavidin bond to *Au* nanowires will be examined.

CHAPTER 2

CURRENT METHODS OF CORTISOL ANALYSIS

The following chapter discusses a few methods utilized to test the levels of cortisol in a sample: Radioimmunoassay (RIA), Competitive Protein Binding Assay (CPB), Fluorometric method, Reverse-phase High Performance Liquid Chromatography, and Electrochemical BioMEMS Cortisol Sensor. The first three are stand-alone applications; they are used to find higher concentrations, and are not very sensitive to minute variations of the hormone in the test sample. Reverse-phase High Performance Liquid Chromatography is described mainly because it aids in the accuracy of the utilized sensor. Finally, electrochemical sensor (described in section 2.5) is a novel way proposed to monitor cortisol hormone levels. Design, fabrication, and method of measurement of this sensor are briefly described. Experimental results from the measurements are outlined and will be used in theoretical analysis in the chapters that follow.

2.1 Radioimmunoassay (RIA)

Developed in 1959, the RIA method can be somewhat dangerous and caution is practiced because it utilizes a radioactive antigen. This procedure utilizes the fact that proteins and antibodies are adsorbed by some plastics (see figure 2.1).

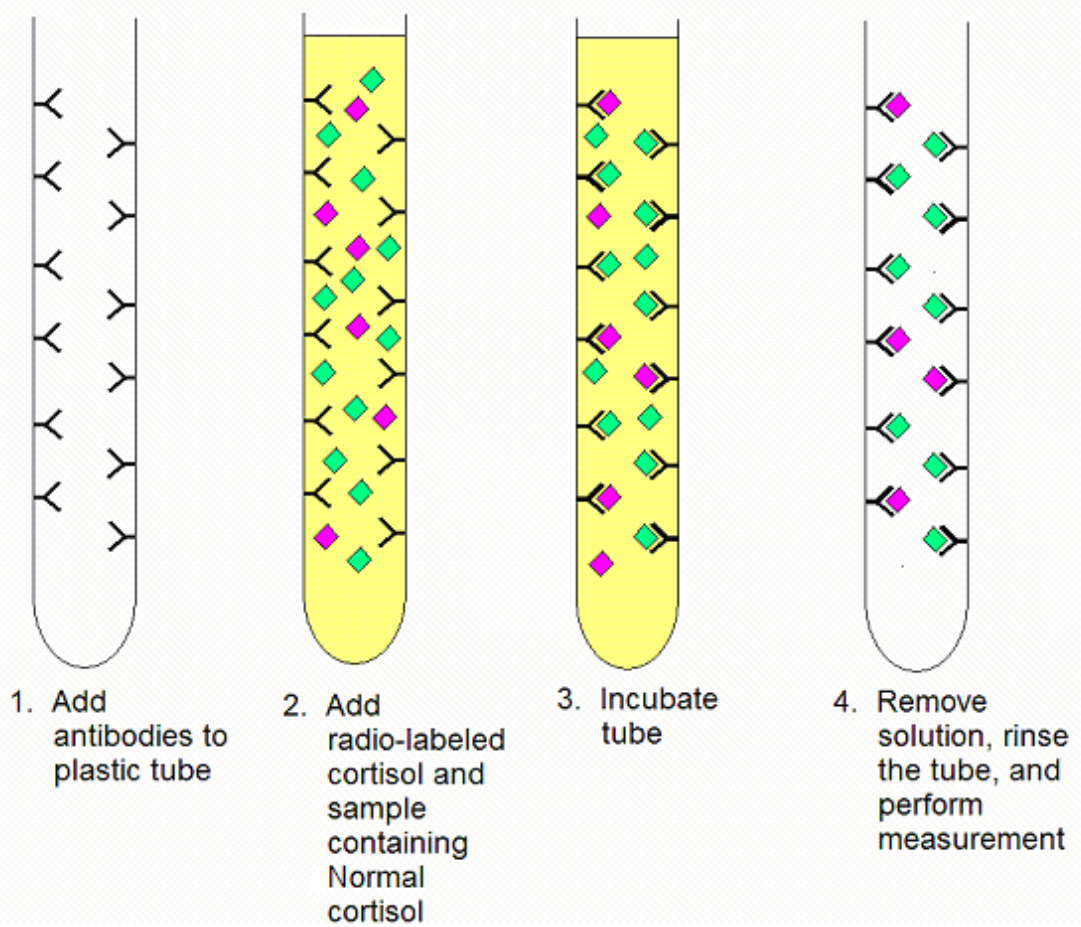

Figure 2.1: Radioimmunoassay

Serum containing the fixed amount of antibodies is added to plastic tubes, and left to incubate for a few minutes for adsorption to take place. Next, the serum is removed and the tube is rinsed with a saline solution, leaving a coat of antibodies on the surface. Solutions containing a fixed number of radioactive cortisol molecules (procedure not described) and test sample are then simultaneously added to the tube, and left to incubate. After incubation, the solutions are removed, and tubes are rinsed. The radioactivity of the tube is then measured depending on the ratio of radio-labeled cortisol and regular cortisol, and the level of normal cortisol in the sample is determined. The radioactivity of

the tube depends on the concentration of cortisol in the test sample since the two attach to a limited number of antibodies in a specific ratio [4, 11].

Even though RIA offers more specificity, it still can lead to erroneous results. A major problem with the RIA cortisol test is that various steroids contained in the sample (along with cortisol) can still react with cortisol antibodies contained in the assay. This can cause false elevations of the cortisol level in the measurement. The measurement is dependent on the antibody used.

To improve the results of the test, it is possible to purify the sample prior to performing an RIA analysis. The process is called chromatography, and it involves extracting specific elements out of the sample for further processing. However, the purification procedure is not always the same and RIA kits are not always the same, either. These variables, combined with research showing that reference levels of cortisol vary between individuals and genders, could make RIA an undesirable method for diagnosing cortisol levels in the system [4, 11].

2.2 Competitive Protein Binding (CPB)

In theory, the CPB and RIA methods are very similar. The major difference between these two methods is the amount of sample needed to perform an analysis, with CPB requiring considerably a smaller amount to perform the analysis. Like RIA, CPB also uses radioactive atoms in order to carry out the measurement and caution is emphasized. The CPB method consists of immobilizing a fixed number of antibodies over a surface to which the cortisol will bind (see figure 2.2).

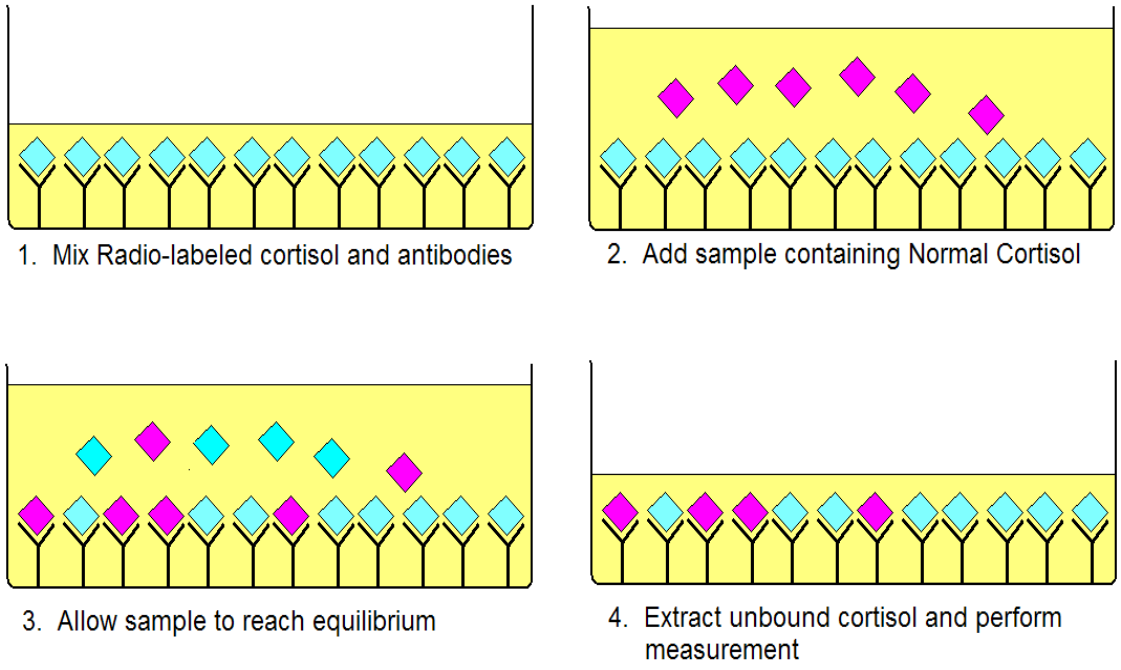

Figure 2.2: Competitive Protein Binding

A fixed amount of cortisol-hormone (labeled with a radioactive atom) is added to bond with antibodies (at this point the radioactivity will reach the peak because all of the radioactive cortisol is present in the sample). The test sample is then added to the assay (already containing bonded radioactive cortisol and antibody). Cortisol from the sample will then proportionally bind to antibodies depending on the ratio to radioactive cortisol. For example, if there are twelve molecules of antibodies and the same number of radioactive cortisol, and we add six molecules of normal cortisol, only four molecules of normal cortisol and eight molecules of radioactive cortisol will bond to the antibodies. Two molecules of normal cortisol and four molecules of radioactive cortisol do not bond and can be separated from the sample by centrifugation or some other method. The radioactivity measurement will then reveal the amount of normal cortisol present since there is an interdependent relation between the two, just like with RIA. Since the cortisol

molecules (normal and radioactive) compete for the binding sites with antibodies, the assay is called Competitive Protein Binding Assay [4, 11].

In practice, the measurements are not so simple and they depend on many other factors. For instance, the specificity of the antibody used may not be very good and other molecules may bind to them. Cortisol-binding protein called transcortin is used as an immobilizing, binding agent. But other hormones such as cortisone, 11-deoxycortisol, and progesterone also have affinity towards transcortin. For this reason, it is recommended to perform chromatography of the test sample before assaying. Further, too small amount of radioactivity may produce erroneous results, thus invalidating the measurement [4, 11].

2.3 Fluorometric Method

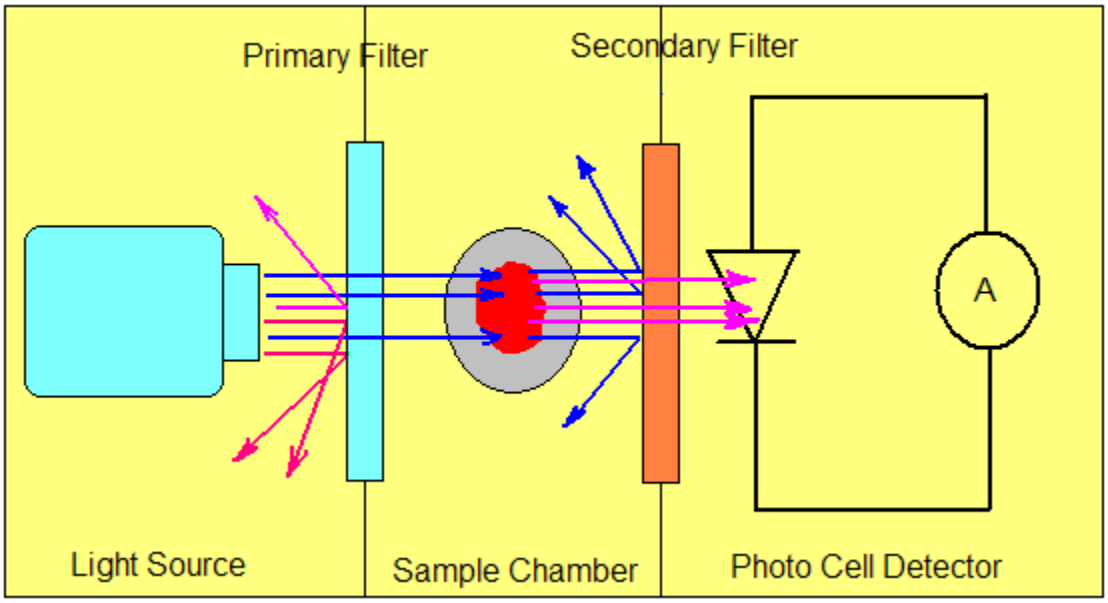

Figure 2.3: Fluorometric Measurement

Fluorescence is a phenomenon that describes the property of certain materials/matter to adsorb light energy and then reemit this light energy in longer wavelengths (less energy). Exciting light usually has to be within a certain range in order to maximize the effect of fluorescence of a certain matter. Likewise, to maximize this effect, fluorometers generally have two filters that separate different light frequencies, only allowing light with a specified wavelength to reach the test sample. The first filter only allows shorter wavelength exciting light to pass through to excite the sample. The second filter serves to filter out scattered exciting light, and only allows filtered light to pass through to the photocell (see figure 2.3).

In order to make use of this assay for cortisol measurements, the hormone must first be extracted and marked with fluorescent reagents. The test sample is first mixed with ethylene dichloride, and shaken rigorously for 20 minutes, in order to enable the attachment of fluorescent reagent to the cortisol hormone. At this point, the sample is centrifuged to separate it from ethylene dichloride. An aliquot of this extract is then placed in a test tube. Fluorescent reagent (absolute ethyl alcohol mixed with concentrated sulfuric acid) is then added to the aliquot extract every 1 minute and vigorously shaken for 20 seconds for binding to take place. After a fixed amount of time, the sample is tested under the fluorometer utilizing a system of two filters described above. For ethyl alcohol mixed with concentrated sulfuric acid marker, the first filter should have a cut-off at 450nm, while the second filter should not pass light lower than 520nm in wavelength.

Although not very specific, the fluorometric assay method can still be used for some clinical tests to determine the level of cortisol. However, like with the previous two

methods, there are factors that can skew the results and thus invalidate the test. It has been noted that large consumption of alcohol and tobacco products can greatly skew the tests. Further, fluorometric instruments can greatly differ between each other. To avoid errors with data comparison due to this reason, it is necessary to establish a reference level (baseline) of the known good sample before measuring the fluorometric response of blood sample or urine sample [4, 11].

2.4 High Performance Liquid Chromatography (HPLC)

The HPLC method was established in late 1960s. This apparatus utilizes six basic components for its operation. These are the liquid mobile phase (also known as carrier liquid), sample injector, mechanical pump (which maintains pressure of the system), column, detector, and data recorder. Depending on the properties of the material being investigated, detection can be performed using refractive index, conductivity, electrochemistry, absorbance or fluorescence.

There are five separation techniques that pertain to liquid chromatography: adsorption, partition, ion-exchange, affinity, and size exclusion chromatography. Of these five, partition is the most popular one and most often used for cortisol analysis. Further, partition is divided into Normal-phase Liquid Chromatography and Reverse-phase Liquid Chromatography (with the latter being used for cortisol separation) [11, 17].

2.4.1 Reverse-phase HPLC (RP HPLC)

Reverse-phase liquid chromatography uses a non-polar stationary phase. This means that as the liquid mobile phase passes through the column carrying the test sample,

undesired elements from the sample are filtered out by the stationary phase. For cortisol, the stationary phase (or the filter) is made up of C_{18} chains that filter small molecules and peptides out of the sample. Finally, when the sample has been properly filtered, it is further passed through a detector of choice, and data graphs are plotted (see figure 2.4).

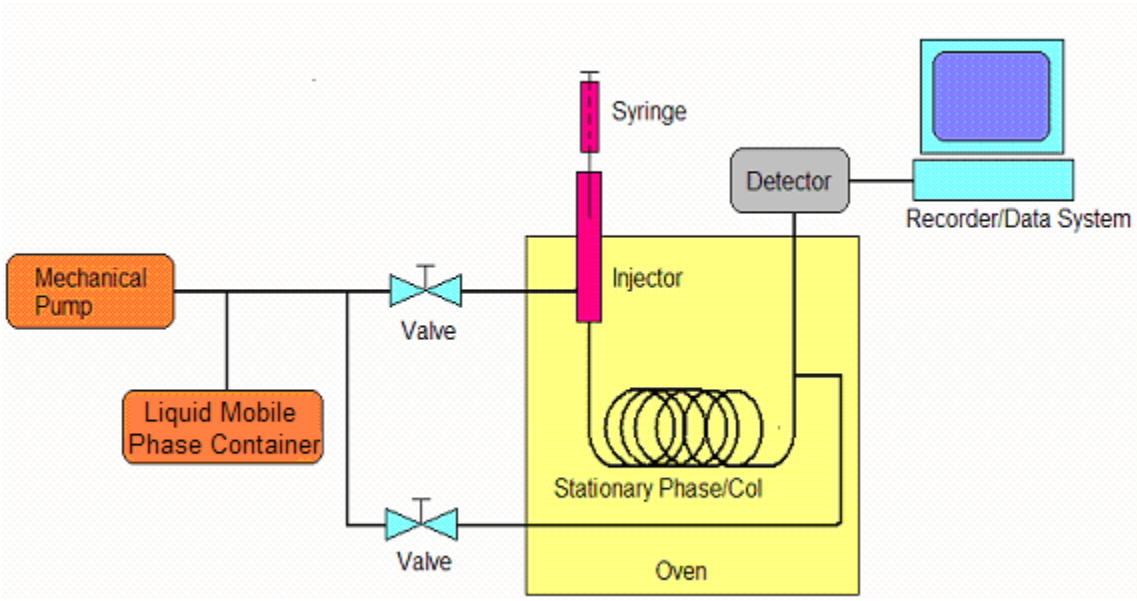

Figure 2.4: High Performance Liquid Chromatograph

Of the four methods for cortisol testing, HPLC seems to offer the best specificity. It seems to be the best option for precise measurements with as little interference from other hormones as possible. Unlike the other three methods, it offers an option of a fully automated process which eliminates the human variable from analysis, resulting in a more precise measurement [11, 17].

2.5 Electrochemical BioMEMS Cortisol Sensor

The electrochemical cortisol sensor is designed and fabricated at the University of South Florida [15] (see figure 2.5). Microelectrodes are first fabricated on the *Si* wafer.

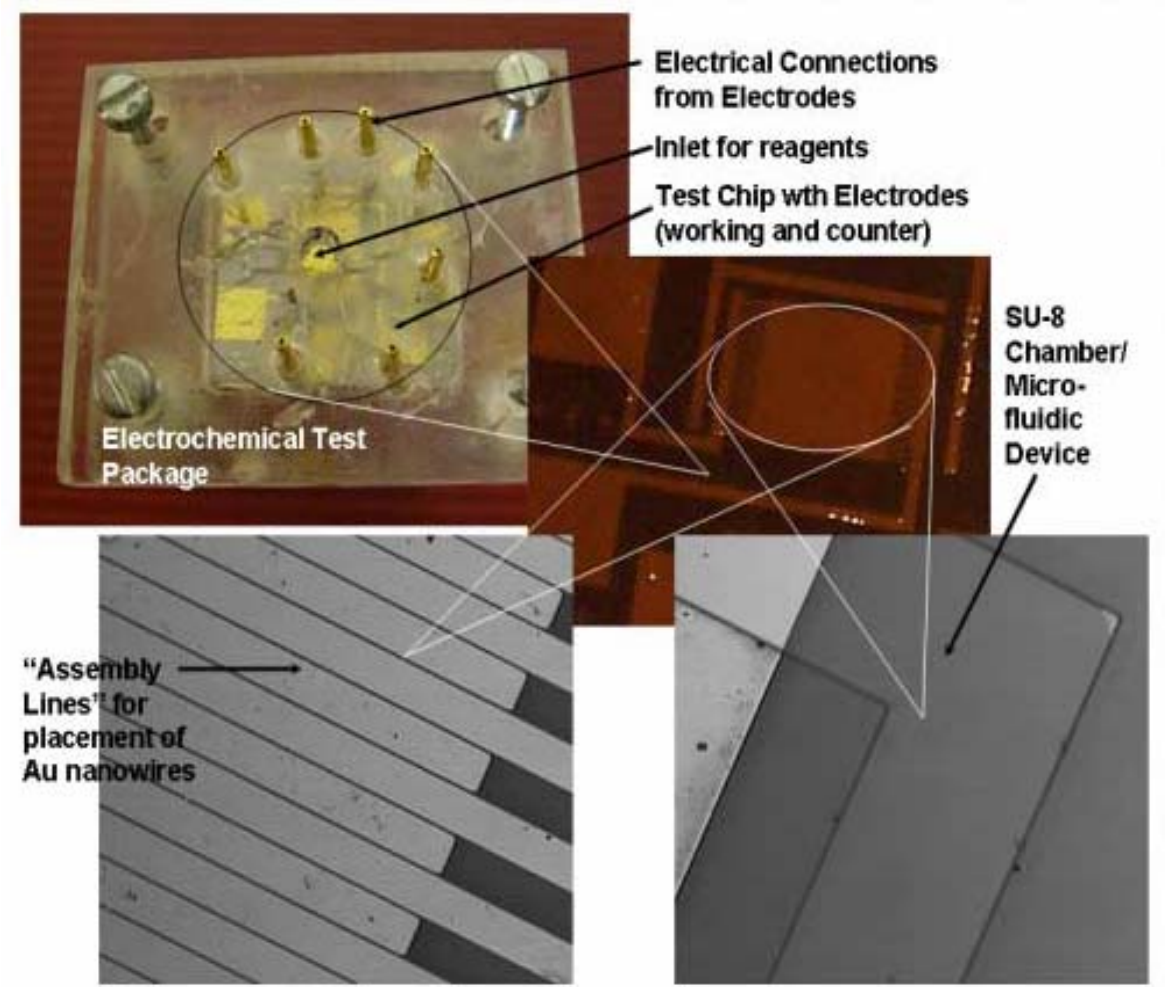

Figure 2.5: Electrochemical BioMEMS Sensor. Reprinted from Biosensors and Bioelectronics, 22, Kumar et al., Ultrasensitive detection of cortisol with enzyme fragment complementation technology using functionalized nanowires, 2138-2144, Copyright (2007), with permission from Elsevier

The working electrode and counter electrode are fabricated by evaporating *Ti* and *Pt* onto the wafer. Afterwards, the *Si* wafer is exposed to a few more lithography steps to fabricate a 60μm tall microfluidic chamber using an *SU-8*. Further, *Au* nanowires are fabricated using a Whatman anodisc template by electroplating in Techni Gold 25 ES solution for one hour. The *Au* nanowires are aligned between the *Pt* electrodes on the surface of *Si* wafer using dielectrophoresis. Cortisol antibodies are then attached to *Au* nanowires utilizing the biotin-streptavidin link added by activation with thioctic acid.

Finally, the electrochemical measurements are performed by mixing 5µl of 0.1M catalyst enzyme 3α-HSD with 25µl of dissolved cortisone at different concentrations. The system is left to react for 5 seconds, and electrochemical measurements are performed (see figure 2.6).

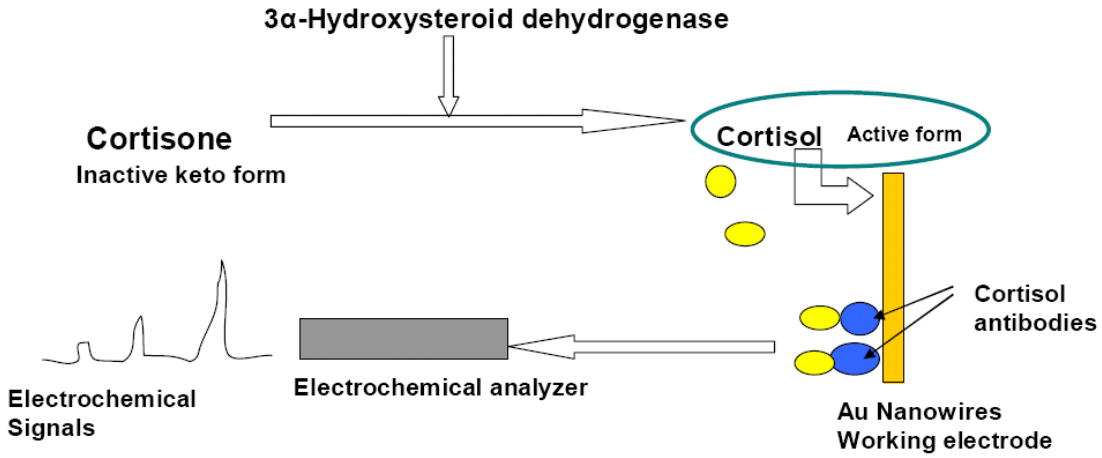

Figure 2.6: Cortisol Detection Scheme. Reprinted from Biosensors and Bioelectronics, 22, Kumar et al., Ultrasensitive detection of cortisol with enzyme fragment complementation technology using functionalized nanowires, 2138-2144, Copyright (2007), with permission from Elsevier

Several scans are performed before the range of the sensor is determined. The increase in current peaks is found to be proportional with the increase in cortisone concentrations. The graph is broken down into two separate entities for clarity (see figure 2.7a and 2.7b). The peak value of current (observed to be at 40mV potential) is afterwards used to calibrate a curve where current is reflected as a function of the concentration of cortisol (see figure 2.8, obtained directly from the authors).

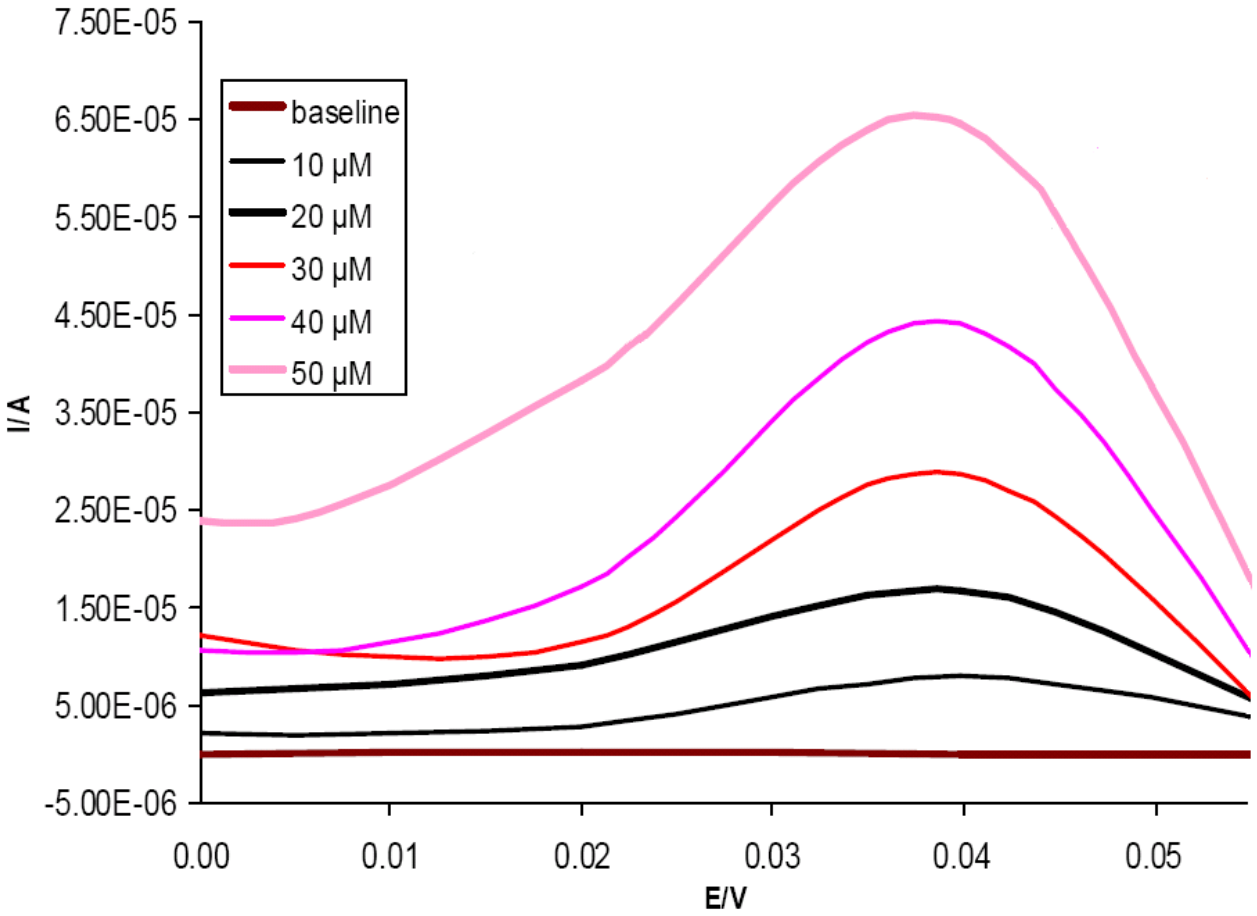

Figure 2.7a: SWV at Different Concentrations of Cortisol (10-50µM). Reprinted from Biosensors and Bioelectronics, 22, Kumar et al., Ultrasensitive detection of cortisol with enzyme fragment complementation technology using functionalized nanowires, 2138-2144, Copyright (2007), with permission from Elsevier

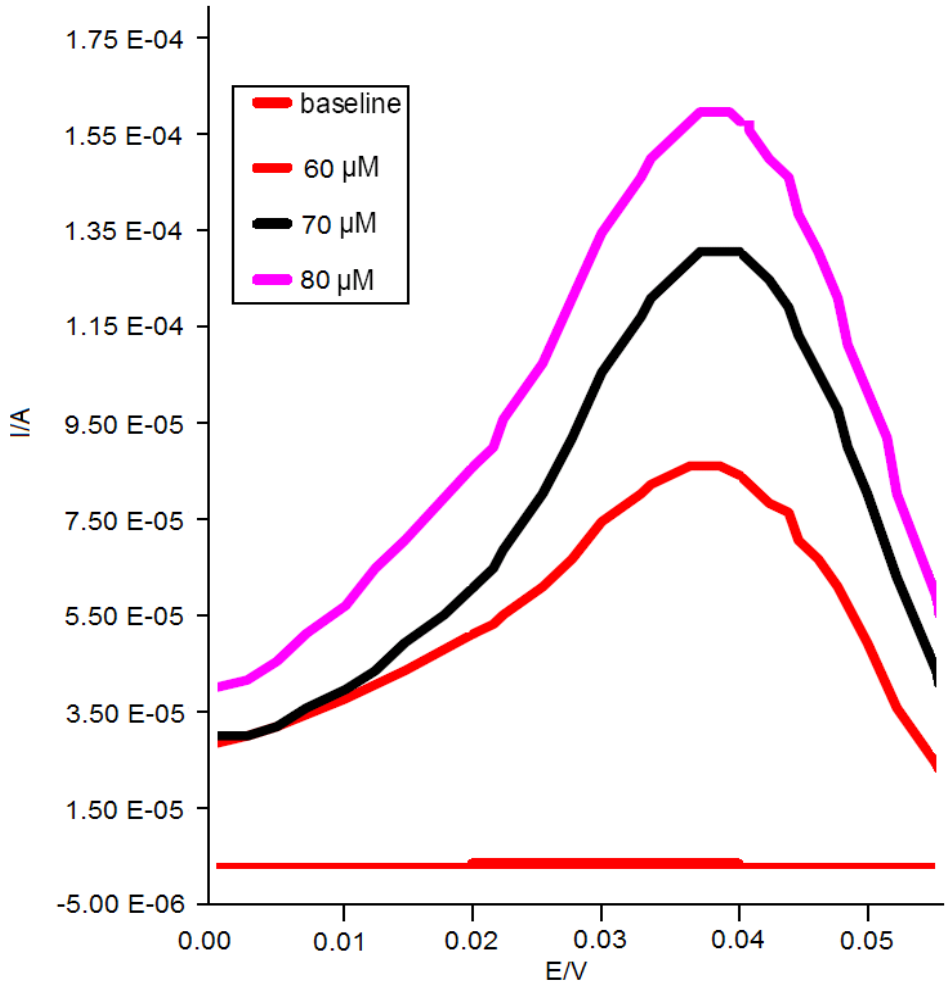

Figure 2.7b: SWV at Different Concentrations of Cortisol (60-80µM). Reprinted from Biosensors and Bioelectronics, 22, Kumar et al., Ultrasensitive detection of cortisol with enzyme fragment complementation technology using functionalized nanowires, 2138-2144, Copyright (2007), with permission from Elsevier

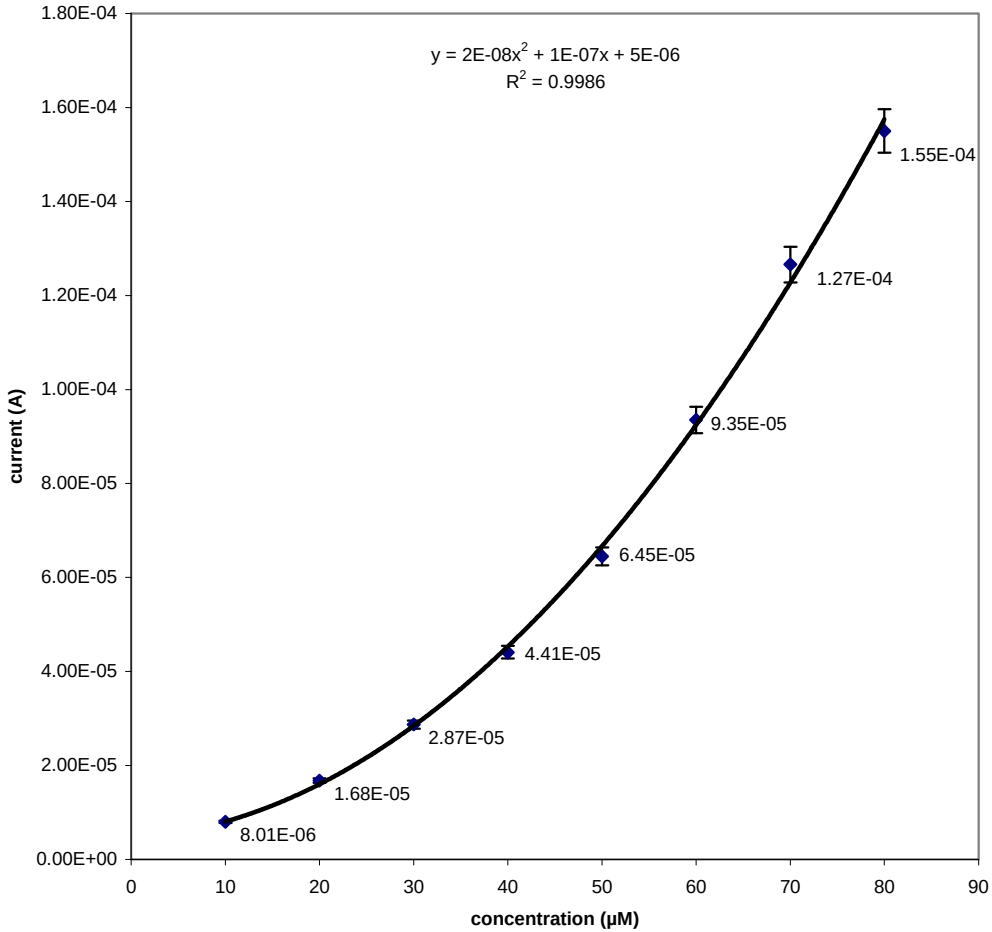

Figure 2.8: Calibration Curve for Cortisol.
Obtained from Arun Kumar, Shyam Aravamudhan, and Shekhar Bhansali. University of South Florida. 2008

CHAPTER 3

THEORY

Chapter 3 introduces the concepts necessary to understand theoretical analysis of the sensor. The first one, dielectrophoresis, is a method used to control the assembly of nanowires as a working electrode of the sensor. The parameters that can be varied to maximize the dielectrophoretic force for ultimate assembly will be discussed. The assembly itself does not seem important at first; however, later it will be shown that a surface area of the working electrode may be an important factor when estimating the total current. The second part of this chapter (introduction to electrochemical measurements) primarily discusses Square Wave Voltammetry (SWV). This helps theoretically confirm and explain the experimental results obtained in the lab.

3.1 Dielectrophoresis

Dielectrophoresis is a scientific method used to align particles in a certain manner using a uniform and/or non-uniform electric field. The subject matter does not need to be charged for the electric field to alter its position. The factors that affect the final result of the alignment of the matter are strength of the electric field, frequency, shape of matter, size of matter, electrical properties of matter, and the medium in which dielectrophoresis

is taking place. The following simplified equation is commonly used to estimate the dielectrophoretic force:

$$F_{DEP} = (m(t) \cdot \nabla E(t)) \tag{3.1}$$

where E is the electric field, m is the dipole moment, and ∇ is the del vector (actual equation includes higher order terms as well as *Maxwell stress tensor*) [5, 25].

As the non-uniform electric field passes from one electrode to the other, it will create a torque on the particle, thus causing it to move. Cylindrically shaped object should therefore align in the same direction of the electric field. The dipole moment induced on the particle can be expressed using the following equation:

$$m(t) = \varepsilon_m V_p K E(t) \tag{3.2}$$

where ε_m is the absolute permittivity of the medium, V_p is the volume of the particle (for cylindrical object $V_p = \pi r^2 l$), E is the electric field, and K is the complex polarization factor. Since the nanowires used for this project are cylindrical in shape, polarizability along the length is more pronounced than either radial orientation. Therefore, complex polarization factor is expressed:

$$K = \frac{\left[\varepsilon_p{}^* - \varepsilon_m{}^*\right]}{\varepsilon_m{}^*} \tag{3.3}$$

where $\varepsilon_p{}^*$ and $\varepsilon_m{}^*$ are complex permittivity of particle and medium respectively. The word *complex* indicates the presence of both *real* and *imaginary* factors, with the latter containing both conductivity σ and angular frequency ω. Therefore, the new equation for the complex permittivity ε^* is:

$$\varepsilon^* = \varepsilon - i\frac{\sigma}{\omega} \tag{3.4}$$

Due to the fact that the E-field and nanowire polarization are in-phase, the dielectrophoretic force can be expressed by looking at the *real* part of equation 3.1, and can therefore be re-written:

$$F_{DEP} = \frac{1}{2}\mathrm{Re}\{m \cdot \nabla E^*\} \tag{3.5}$$

Combining equations 3.2 and 3.5 yields a new expression for dielectrophoretic force, and is written:

$$F_{DEP} = \frac{1}{2}\pi r^2 l \varepsilon_m \,\mathrm{Re}\{K\} \nabla \mid E_{rms} \mid^2 \tag{3.6}$$

Root mean square value of the electric field E_{rms} as well as complex polarization factor K can further be broken down as following:

$$\nabla \mid E_{rms} \mid^2 = \left| \frac{dV_{rms}}{dx} \nabla_x \left(\frac{dV_{rms}}{dx} \right) \right| \tag{3.7}$$

$$\mathrm{Re}\{K\} = \frac{\omega^2 \left(\varepsilon_m \varepsilon_p - \varepsilon_m{}^2 \right) + \left(\sigma_m \sigma_p - \sigma_m{}^2 \right)}{\varepsilon_m{}^2 \omega^2 + \sigma_m{}^2} \tag{3.8}$$

Finally, equation 3.6 can be combined with equations 3.7 and 3.8 to yield the final equation of the dielectrophoretic force:

$$F_{DEP} = \left(\frac{1}{2}\pi r^2 l \varepsilon_m \right) \left(\frac{\omega^2 \left(\varepsilon_m \varepsilon_p - \varepsilon_m{}^2 \right) + \left(\sigma_m \sigma_p - \sigma_m{}^2 \right)}{\varepsilon_m{}^2 \omega^2 + \sigma_m{}^2} \right) \left| \frac{dV_{rms}}{dx} \nabla_x \left(\frac{dV_{rms}}{dx} \right) \right| \tag{3.9}$$

Upon the alignment of each nanowire between electrodes, the magnitude of the electric field between electrodes is reduced. Depending on the application, this can create a serious issue because a majority of nanowires can end up being scattered, randomly melting and welding to the electrode. If nanowires are going to be used as a

working electrode for electrochemical measurements (like in this project), it becomes more complicated to estimate the true surface area of the working electrode. The exact value of the surface area in this case is necessary for final data analysis and estimation.

At frequencies below 1kHz nanowires may have a tendency to evaporate, further complicating the above problem. Evaporation does not seem to be the problem at higher frequencies. At 10kHz or higher, the strength of the dielectrophoretic force seems to be weaker [25].

On the other hand, the same strength of the dielectrophoretic force is exponentially proportional to the peak voltage applied across the electrodes. In short, to manipulate/maximize the strength of the force, voltage and frequency are the two variables most commonly altered to tweak the force as desired. The user may not have much choice with the permittivity due to the fact that different liquids/buffers may force an unpredicted reaction in a sensor itself, thus skewing results.

Further, it is thought that dielectrophoresis is applicable to structures between 1 and 1000μm. Gravity is suspected to be a major interference for structures larger than 1000μm. For small structures under 1μm in size, Brownian motion (random movement of particles suspended in liquid) overwhelms the DEP force [5, 25].

3.2 Electrochemistry

By definition, electrochemistry is the study of the interchange of chemical(s) and electric current. There are different types of electrochemical measurements, but for this project Square Wave Voltammetry (SWV) was used, and therefore will be discussed. This method utilizes a system of three electrodes to provide an excitation voltage, and

measure the current from the electrochemical cell: working electrode (WE), reference electrode (RE), and counter electrode (CE) [2, 3, 13, 20, 30, 35].

3.2.1 Electrode Function Breakdown

Working electrode (WE) is where all the electrochemical changes occur. In other words, it is a point where the apparatus provides electrical excitation and performs measurements with respect to the reference electrode and the counter electrode.

Reference electrode (RE) is the electrode of a fixed, constant potential with respect to the electrolyte and is kept at equilibrium. The potential of the RE serves as a reference when measuring the potential of the WE. Because of the need to keep the RE at equilibrium, it is not recommended to pass charge through it. Most reference electrodes contain the chemical element *Cl*, and current flow will cause the concentration to fluctuate. Finally, the counter electrode (CE) is included to facilitate the passage of current at the WE [2, 3, 13, 20, 30, 35].

3.2.2 Fundamentals of Electrochemistry

To reflect on some fundamentals and terminology in electrochemistry, it is imperative to start with the term of equilibrium. In electrochemistry, equilibrium means zero current during potentiometric measurement. In other words, it is common to say that a system in equilibrium has an absent power source driving the reaction (effectively equivalent to an open circuit - electronic wise). However, even though the current does not exist between the electrodes, the electrodes still have some potential. This potential is equilibrium electrode potential and very important when determining the overpotential of

an electrode, which is the difference between new electrode potential and its equilibrium equivalent while forcing charge.

$$\eta = E_{electrode} - E_{equilibrium} \tag{3.10}$$

When forcing the charge on the electrode, the equilibrium of the system will be disturbed, thus resulting in varying the electrode potential. At this point, the flow of charge is accompanied with electron uptake (reduction) or electron loss (oxidation) of the electroactive analyte in the electrolyte by the working electrode, thus changing the concentration and activities of the analyte in the electrolyte. Activity and concentration are closely related. Activity is defined as concentration perceived by electrode, and is expressed by:

$$a = c * \gamma \tag{3.11}$$

(where a is activity, c is concentration, and γ is activity coefficient). However, at low concentrations, this γ is considered equal to unity, and the new form of equation is:

$$a = c \tag{3.12}$$

Altering this ratio of activities at the electrode/solution interface and conversion of the material from reduced to oxidized form and back will in turn result in production/consumption of charge. This phenomenon is somewhat described by a form of the Nernst equation:

$$E_{working\,electrode} = E^0 + \frac{RT}{nF} \ln \frac{a_{Ox}^{(@electrode\ surface)}}{a_{\mathrm{Red}}^{(@electrode\ surface)}} \tag{3.13}$$

(E^0 is standard electrode potential, R is universal gas constant (8.314510 J K^{-1} mol^{-1}), T is temperature (in Kelvin), n is number of electrons involved in reaction, F is Faraday constant (9.6485309×10^4 C mol^{-1}), and a_{Ox} and a_{Red} are chemical activities for the

oxidized and reduced species respectively). The true Nernst Equation is only valid when the system is in equilibrium, and is:

$$E_{equilibrium} = E^0 + \frac{RT}{nF} \ln \frac{a_{Ox}^{(@\,electrode\ surface)}}{a_{\mathrm{Re}d}^{(@\,electrode\ surface)}} \qquad 3.13a$$

Under this condition net current density is equal to either forward or reverse current of the reaction:

$$I_{net} = I_{forward} = I_{reverse} \qquad 3.14$$

Forward current (also known as oxidative or anodic current) is obtained when a species of interest loses electrons. Likewise, reverse current (also known as reductive or cathodic current) is obtained when a species of interest gains electrons. It can be mathematically shown that the Nernst equation is therefore a derivative of the above equation (and vice versa). However, equation 3.13 is a "form" of the Nernst equation because the system is not in equilibrium. When the system is not in equilibrium, forward and reverse currents are not the same, and net current is the addition of the two.

$$I_{net} = I_{forward} - I_{reverse} \qquad 3.15$$

In practice, the currents flow opposite to one another, so to account for that, a negative sign is used in the formula. Following formulas are adopted for forward and reverse currents:

$$I_{forward} = I_0 a_{Ox} e^{\left(\frac{(1-\alpha)nF(E-E_{equilibrium})}{RT}\right)} \qquad 3.16$$

$$I_{reverse} = I_0 a_{\mathrm{Re}d}\, e^{\left(\frac{-\alpha nF(E-E_{equilibrium})}{RT}\right)} \qquad 3.17$$

(α is a transfer coefficient, and in most cases has a value of 0.5). The term I_0 is also known as exchange current. It is calculated by multiplying the exchange current density i_0 [A/m^2] with total surface area of a working electrode A[m^2]. This is the rate constant of electron transfer while the system as a whole is in equilibrium.

Combining the equations 3.15, 3.16, and 3.17, the final equation for estimating the net current is obtained:

$$I_{net} = I_0 \left[a_{Ox} e^{\left(\frac{(1-\alpha) nF (E - E_{equilibrium})}{RT} \right)} - a_{\mathrm{Re}\,d} e^{\left(\frac{-\alpha nF (E - E_{equilibrium})}{RT} \right)} \right] \qquad 3.18$$

The above equation is the Butler-Volmer equation and it may be used to estimate the total current at any particular instance. Finally, to conclude this part of the chapter, it is important to emphasize that the above theory is not always useful when predicting forward and reverse currents. The graphical representation of the above currents has a form as in figure 3.1 below, and currents do not peak [2, 3, 13, 20, 30, 35].

The method of measurement used for this experiment, Square Wave Voltammetry, significantly differs from figure 3.1 in output. Square Wave Voltammetry is characterized by forward and reverse current graphs that reach a peak at one point, and converge to a fixed value on either end. This method is briefly described in the following section.

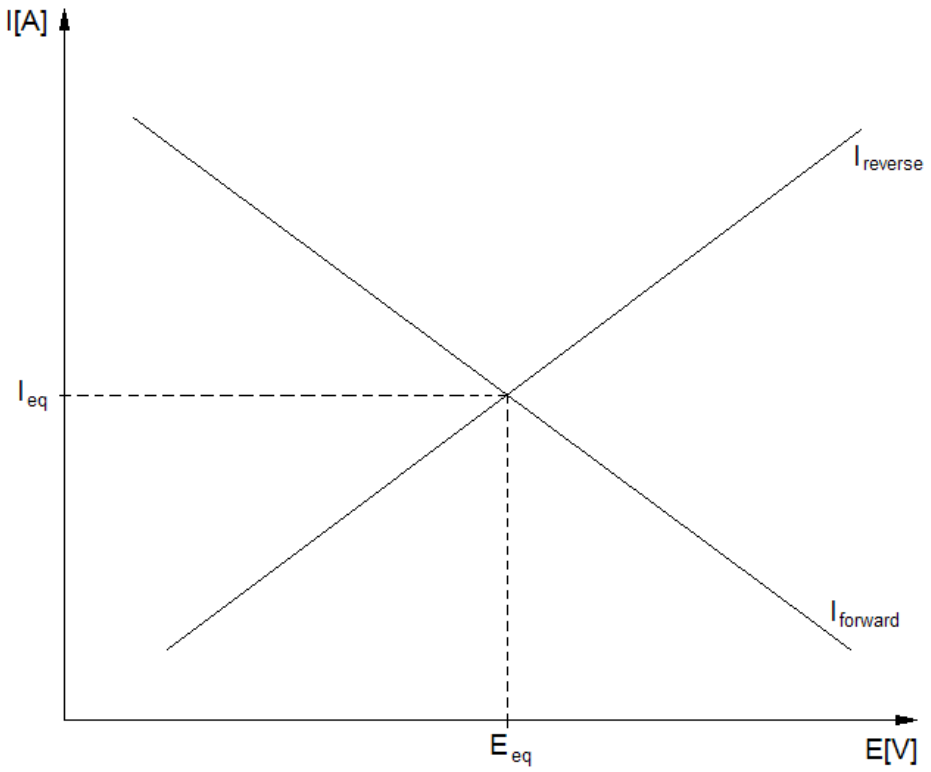

Figure 3.1: Forward and Reverse Current in El-Chem System

3.2.3 Square Wave Voltammetry (SWV)

Electrochemical voltammetry is a method where voltage is varied over a time period, while at the same instance, current is measured in a reaction. The square wave excitation signal applied to the working electrode (WE) is shown in figure 3.2. Voltage pulses are applied at a user directed rate ν (Vs^{-1}) and period τ (ms). ΔE_p is usually 50mV, ΔE_s is commonly about 5mV, and t_p is usually anywhere between 20-40ms.

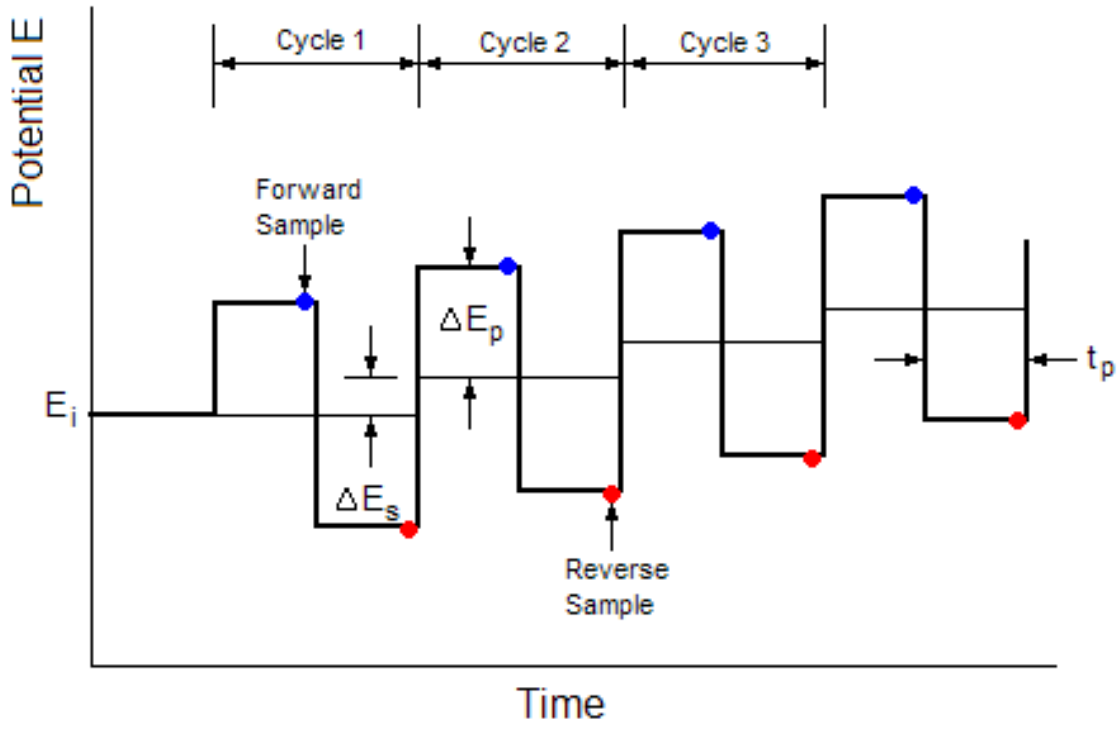

Figure 3.2: Time-Potential Profile for SWV. Electrochemical Methods – Fundamentals and Applications. Allen J. Bard & Larry R. Faulkner. David Harris, Elizabeth Swain & Eugene Aiello. Copyright (2001) John Wiley & Sons, Inc. Reprinted with permission of John Wiley & Sons, Inc.

While the voltage on the working electrode (WE) is applied, the current measurements are performed by the apparatus first in the forward, then in the reverse direction. The net current is the addition (or difference) between these two currents, and the net current is the one reflected on the monitor of the instrument. An example of one such reading is illustrated in figure 3.3.

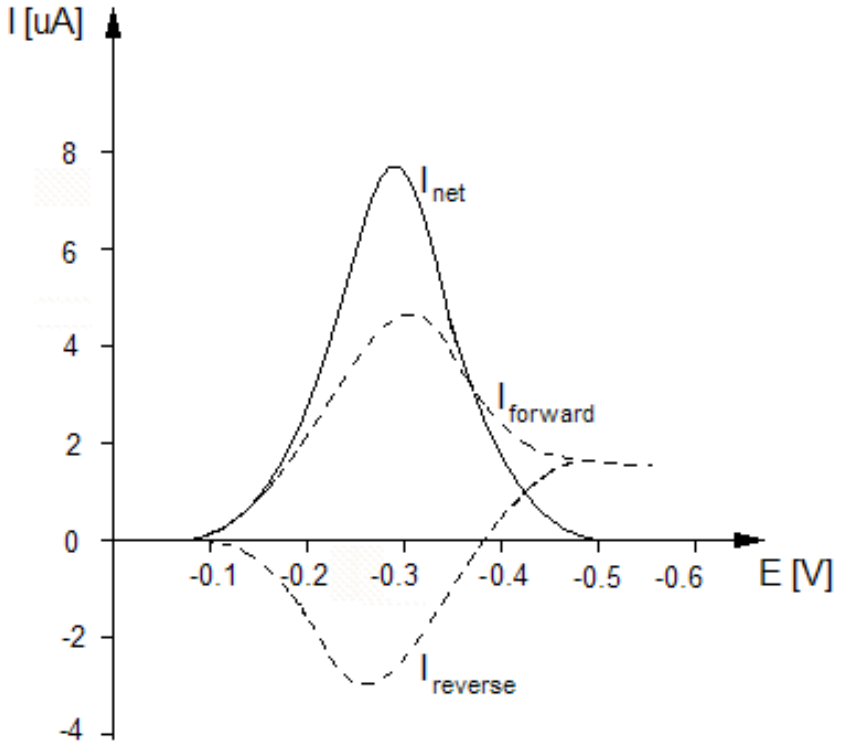

Figure 3.3: Square Wave Voltammogram. Reprinted with permission from (Anal. Chem., Vol: 49, No.: 13, 1904-1908). Copyright (1977) American Chemical Society.

A few equations are utilized to describe the SWV waveform. First, depending on the selected parameters, potential waveform is applied to the working electrode, and is described as:

$$E_m = E_i - \left[Int\left(\frac{m+1}{2}\right) - 1 \right] \Delta E_s + (-1)^m \Delta E_p \quad (for\ m \geq 1) \tag{3.19}$$

(where m denotes a series of half cycles from the first forward pulse (m = 1), and Int[(m=1)/2] denotes truncation of the ratio to the highest integer). The balance of the concentrations of oxidative and reductive species at the surface of the working electrode (also known as Nernstian balance) is then described as:

$$\theta_m = \frac{C_O(0,t)}{C_R(0,t)} = \exp\left[\frac{nF}{RT}(E_m - E_{1/2})\right] \tag{3.20}$$

(where *n* is the number of electrons involved). The above equation provides an input for calculating another parameter required for estimation of total current.

$$Q_i = \frac{\xi\theta_i}{1+\xi\theta_i} \quad (i > 0) \quad Q_0 = 1 \tag{3.21}$$

$$\xi = \left(\frac{D_O}{D_R}\right)^{0.5} \tag{3.22}$$

(where D_O is the diffusion coefficient of the O-species, and D_R is the diffusion coefficient of the R-species).

In Square Wave Voltammetry (SWV), current is expressed as a dimensionless unit ψ. Since in every cycle, there is one forward current sample and one reverse current sample obtained, the total forward and reverse current will be the addition of all the previous (preceding) half cycles, and the present one. Therefore, the dimensionless current equation is expressed as:

$$\psi_m = \sum_{i=1}^{m} \frac{Q_{i-1} - Q_i}{(m-i+1)^{0.5}} \tag{3.23}$$

where odd values of *m* correspond to forward current, while even values correspond to reverse current samples. Finally, the dimensionless current difference (analogous to net current from equation 3.18) is written as:

$$\Delta\psi_m = \psi_m - \psi_{m+1} \tag{3.24}$$

where *m* covers only odd values, and odd *m* is taken first. The dimensionless current Voltammogram is illustrated in figure 3.4 below (not to be confused with figure 3.3 that

represents the response of a particular sensor measured in amperes. $E_{1/2}$ is very close to $E^{0'}$, and is expressed by equation $E_{1/2} = E^{0'} + \frac{RT}{nF} \ln\left(\sqrt{\frac{D_R}{D_O}}\right)$.

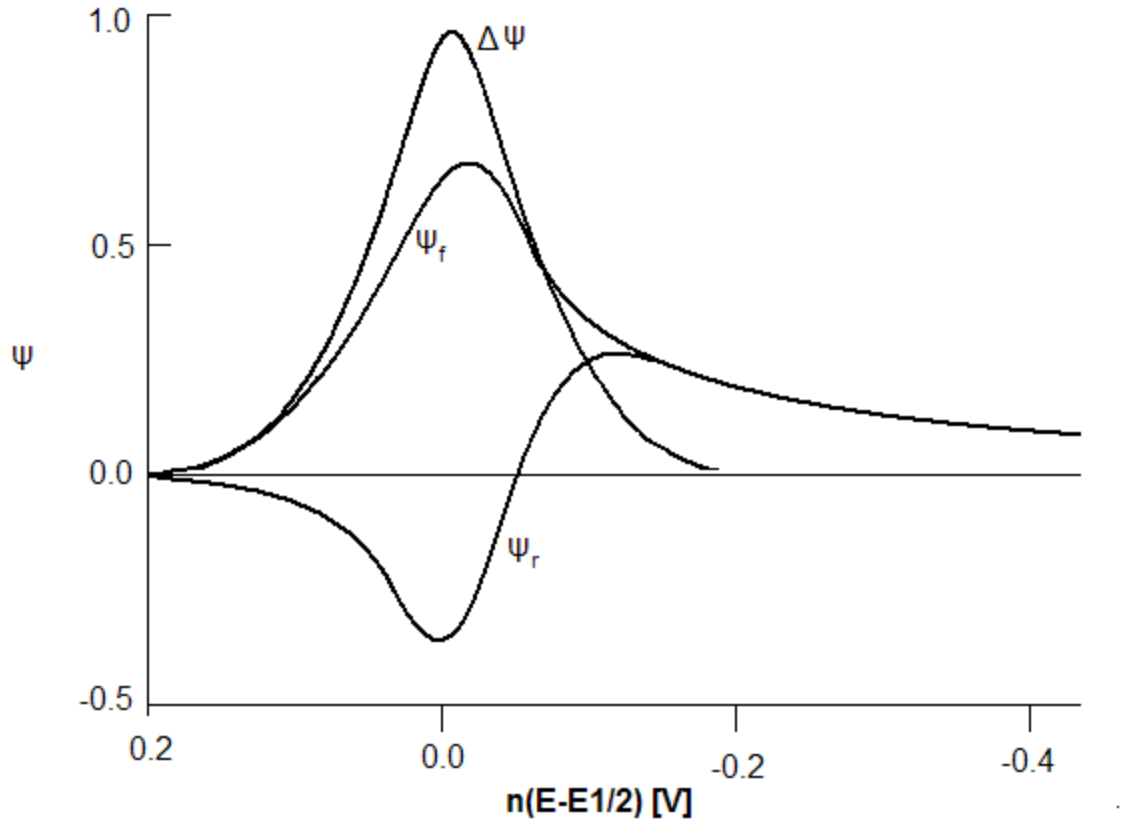

Figure 3.4: Dimensionless Current. Reprinted with permission from (Anal. Chem., Vol: 53, No.: 4, 695-701). Copyright (1981) American Chemical Society.

Determining the peak reflects the peak dimensionless current $\Delta\psi_p$ from figure 3.4, which enables estimation of the peak of the current according to equation 3.25:

$$\Delta i_p = \frac{nFAD_O^{0.5} C_O^*}{\pi^{0.5} t_p^{0.5}} \Delta\psi_p \qquad 3.25$$

(where C_O^* is the bulk concentration of O-species). An important fact to note is that difference peak current $\Delta\psi_p$ happens near the half wave potential $E_{1/2}$, which has to be taken into account when graphing the final current waveform versus potential.

Current equals 0 when the forced potential is much larger than $E_{1/2}$. Since the forced potential is far away from the electrolysis point, the forward and reverse current do not flow. When the forced potential starts approaching $E_{1/2}$, electrolysis starts to occur and forward and reverse currents start to flow. Finally, when the forced potential becomes much smaller than $E_{1/2}$, electrolysis happens at the diffusion controlled rate independent of the applied potential and both forward and reverse current become similar [1-3, 13, 20, 22, 26-28, 30, 33-35].

The peak of dimensionless current is also dependent on square wave parameters. From table 3.1 it is evident that peak is dependent and increases with ΔE_p and ΔE_s. The value of $\Delta\psi_p$ can then be used to estimate other unknown parameters from equation 3.25.

Table 3.1: Dimensionless Peak Current vs. SWV Operating Parameters. Electrochemical Methods – Fundamentals and Applications. Allen J. Bard & Larry R. Faulkner. David Harris, Elizabeth Swain & Eugene Aiello. Copyright (2001) John Wiley & Sons, Inc. Reprinted with permission of John Wiley & Sons, Inc.

$n\Delta E_p$ /mV	**$n\Delta E_S$ /mV**			
	1	**5**	**10**	**20**
10	0.2376	0.2549	0.2726	0.2998
20	0.4531	0.4686	0.4845	0.5077
50	0.9098	0.9186	0.9281	0.9432
100	1.1619	1.1643	1.1675	1.1745

Table 3.1 is helpful in estimating a single peak point of the current, but equation 3.23 has to be incorporated in order to see how the current really behaves over a larger range of voltage. So, the current for the m^{th} half-cycle is:

$$i_m = \frac{nFAD_O^{0.5}C_O^*}{\pi^{0.5}t_p^{0.5}} \sum_{i=1}^{m} \frac{Q_{i-1} - Q_i}{(m-i+1)^{0.5}} \tag{3.26}$$

Again, an important thing to note about this equation is that odd values of *m* correspond to forward current, and even correspond to reverse current. Net current is the difference between the forward and reverse samples shown in:

$$\Delta i_m = i_m - i_{m+1} \tag{3.27}$$

(where *m* covers only odd values, and odd *m* is taken first). Further, the diffusion coefficient is described in terms of the radius of the moving particles and molecules in the solvent by equation:

$$D = \frac{RT}{6\pi N \nu r} \tag{3.28}$$

(where *v* is the viscosity of the solvent, *N* is Avogadro's number, and *r* represents the radius of a molecule/particle) [1]. The radius is then described by Stokes radius (which is the equivalent of the radius of a hard sphere that diffuses at the same rate as an actual molecule) in equation 3.29:

$$r = \sqrt[3]{\frac{3V}{4\pi}} \tag{3.29}$$

(where V is a cell volume of a particle/molecule).

Square Wave Voltammetry (SWV) features a number of advantages when compared to other methods. From figure 3.3 it can be seen that since the peak value is

the addition of two currents and therefore larger, the value of the current is more easily estimated (hence, increasing the accuracy). Further, Square Wave Voltammetry (SWV) minimizes the capacitive contributions to the overall current, resulting in dramatic increase of scan rate (capacitive current is always present as long as there is AC excitation on the electrode. Keeping the excitation signal constant greatly reduces the capacitive effect. For this reason, current measurements are performed right before the potential changes in order to minimize the capacitive effect). Finally, the height of the peak of the net current is directly proportional to the concentration of analyte, making the interpretation of the results easier [1-3, 13, 20, 22, 26-28, 30, 33-35].

3.2.4 Construction of Electrochemical Cell

The next step is the construction of the cell where the measurements will take place. This is a simple yet complicated process, due to so many rules to follow, and the greatest challenge is trying to satisfy all of the requirements. Only a few important rules are mentioned and implemented for the sake of this experiment, and will later be discussed.

The very first rule states that the tip of the RE should be positioned as close as possible to the surface area of the WE. This minimizes the ohmic drop and polarization of the WE should be uniform. Second, the CE should be positioned downstream from the WE, and it is recommended that the CE be excluded from the solution bulk or significantly away from it, but still in contact with main body of the cell. The reason for this is because the CE reaction with the electrolyte may produce negative effects on the

measurement. Finally, one last rule of utmost importance is to thermally isolate the cell because the reactions are temperature dependent [2, 3, 13, 20, 30, 35].

Failure to satisfy these few rules can greatly skew the results. But again, these are just a few requirements to keep in mind. The design could get expensive and labor-intensive if all requirements were to be satisfied, especially if the cell had to be dimensionally small. One possible scheme for constructing the electrochemical cell is illustrated in figure 3.5 below.

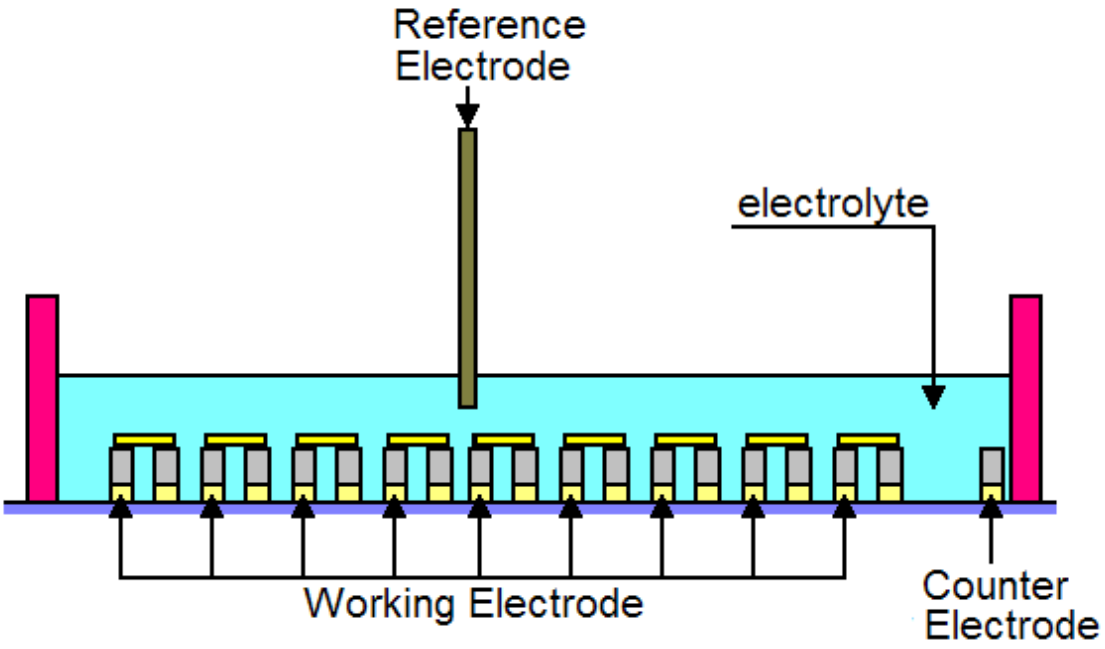

Figure 3.5: Graphical Representation of El-Chem Cell

Upon completing the cell, the electrodes are connected to the apparatus and electrochemical measurements of choice are performed. Figure 3.6 below depicts a block diagram of such an apparatus [2, 3, 13, 20, 30, 35].

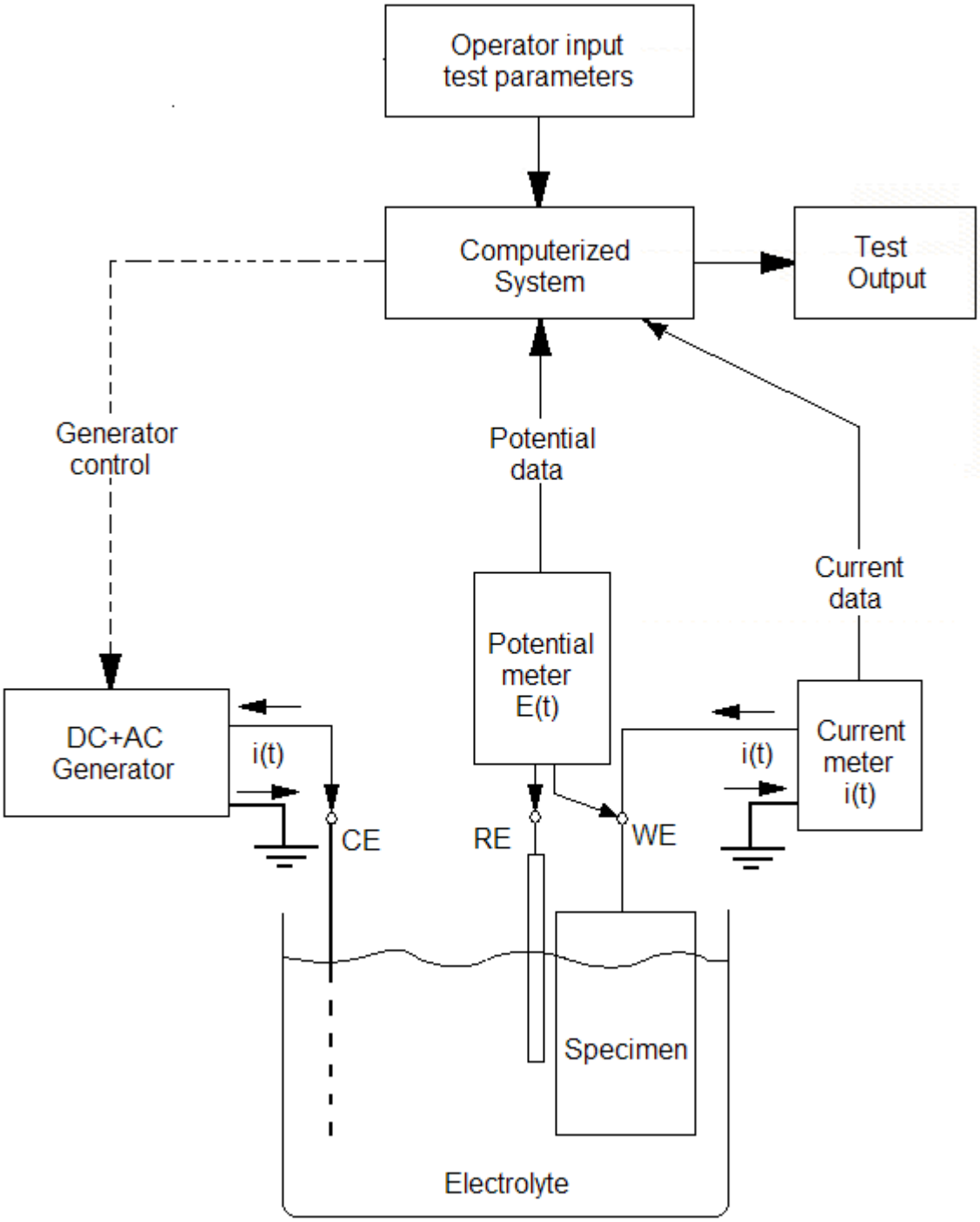

Figure 3.6: Block Diagram of Apparatus for El-Chem Analysis.
Adapted from class notes. A. Sagues. Electrochemical Diagnostic Techniques. 2006

CHAPTER 4

RESULTS

This chapter attempts to give an explanation to the experimental results shown in section 2.6. It is necessary to refer back to chapter 3 equations (3.19 – 3.29) in order to calculate the peak current for a given concentration of cortisone/cortisol using the SWV measurement method. First, looking at equation 3.26, a few unknown quantities are left to be determined.

$$i_m = \frac{nFAD_O^{0.5}C_O^*}{\pi^{0.5}t_p^{0.5}} \sum_{i=1}^{m} \frac{Q_{i-1} - Q_i}{(m-i+1)^{0.5}} \qquad 3.26$$

The oxidative and reductive species diffusion coefficient, dimensionless current (summation term), and the surface area of the working electrode are for now unknown. The following section explains the approach taken to estimate the diffusion coefficient of the oxidative and reductive species – cortisone and cortisol.

4.1 Calculation of Diffusion Coefficients

Diffusion coefficients were estimated using equation 3.28. Since the reaction takes place in phosphate buffer saline (PBS), which has properties similar to water, viscosity of water $0.001\left[\frac{Ns}{m^2}\right]$ is therefore used for this equation.

$$D = \frac{RT}{6\pi N v r} \tag{3.28}$$

The value of the radius for equation 3.28 is obtained from equation 3.29. The unit cell volume for equation 3.29 is obtained from the Cambridge Structural Database [6, 29] for both cortisone and cortisol.

$$r = \sqrt[3]{\frac{3V}{4\pi}} \tag{3.29}$$

The software patch for cortisone molecule is downloaded from the Cambridge Structural Database. This software patch is uploaded into Mercury software (also obtained from the Cambridge Structural Database), which enables viewing of all the structural and physical information of the cortisone molecule (see figures 4.1a, 4.1b, and 4.1c below). An important thing to stress is that cell volume is expressed as a volume of a rectangular prism that a single molecule occupies.

Since molecules are not spherical in shape, the radius of the molecule is then the radius of a perfect sphere that diffuses at the same rate as the actual molecule, also known as Stokes radius. Therefore, the volume of a rectangular prism is equated to the volume of a perfect sphere. The rectangular prism volume (see figure 4.1c) is incorporated into equation 3.29, upon which the final value for the Stokes radius of the cortisone molecule is obtained.

$$r = \sqrt[3]{\frac{3*1838.22}{4*\pi}} = 7.60*10^{-10}\,[m]$$

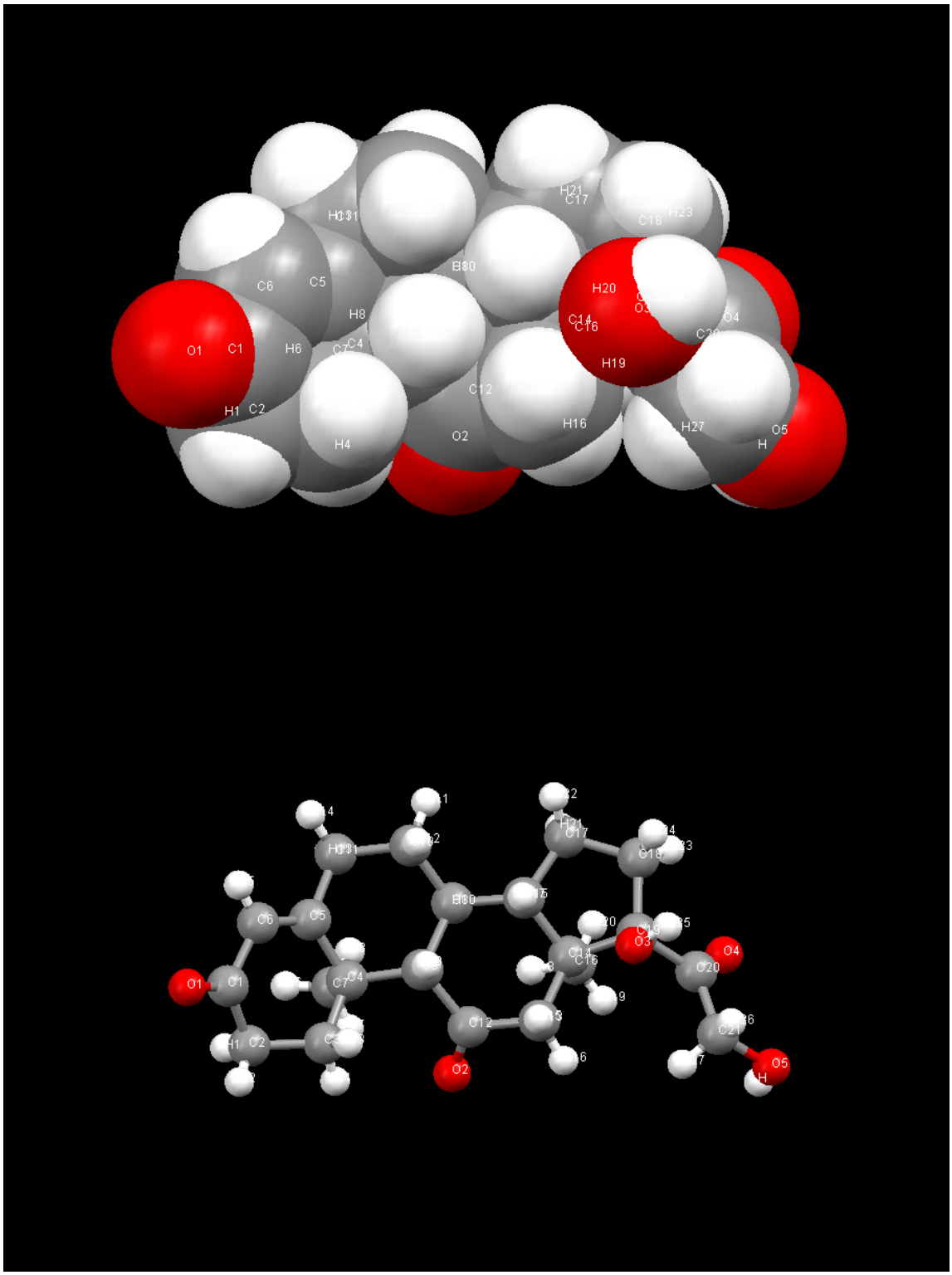

Figure 4.1a: Views of Cortisone Molecule. Mercury Software from Cambridge Structural Database. [http://www.ccdc.cam.ac.uk/support/product_references/]

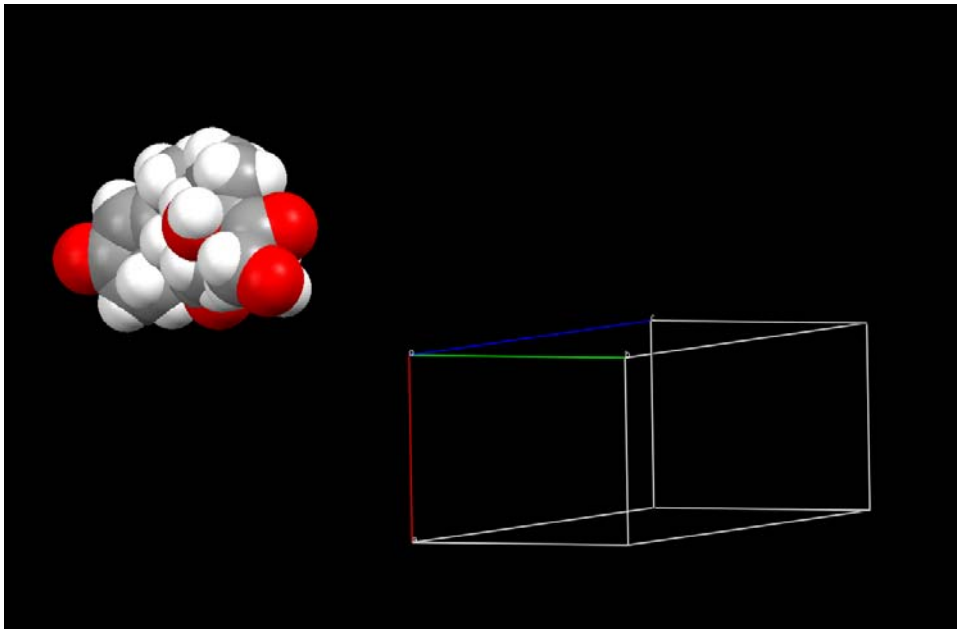

Figure 4.1b: Rectangular Prism Unit Cell. Mercury Software from Cambridge Structural Database. [http://www.ccdc.cam.ac.uk/support/product_references/]

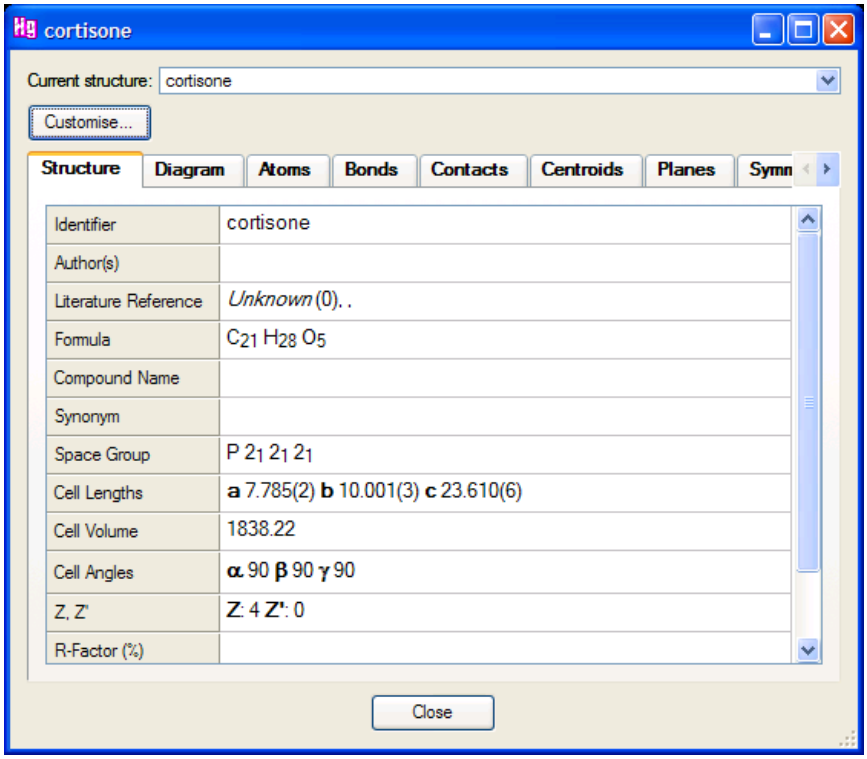

Figure 4.1c: Structural Info of One Molecule of Cortisone. Mercury Software from Cambridge Structural Database. [http://www.ccdc.cam.ac.uk/support/product_references/]

The radius of a single cortisone molecule is estimated to be approximately 7.6Å. Incorporating this value into equation 3.28, the diffusion coefficient for cortisone (oxidative species) is calculated to be:

$$D=\frac{RT}{6\pi N\nu r}=\frac{8.314\left[\frac{J}{K\cdot mol}\right]*298.15[K]}{6*\pi*6.022*10^{23}\left[\frac{1}{mol}\right]*0.001\left[\frac{N\cdot s}{m^2}\right]*7.6*10^{-10}[m]}\approx 2.87*10^{-10}\left[\frac{m^2}{s}\right]$$

The dimensions of a unit cell for cortisol (a = 6.435Å, b = 15.626Å, c = 18.912Å) yield a cell volume of 1901.67Å^3 [6]. Using the equivalent calculation procedure described above yields the radius of a single cortisol molecule (reductive species) to be approximately 7.69Å. The diffusion coefficient of cortisol is calculated to be 2.84*10^{-10} m^2/s.

Of course, the calculations above represent rough estimates of what the true value of both diffusion coefficients are. The molecules are too small to precisely calculate their volume. Further, the value of the diffusion coefficient greatly depends on the environment in which the measurements are performed. The viscosity of PBS, for example, is not available from a manufacturers' specification sheet. The viscosity of water is used instead, even though the two mediums may slightly differ in this aspect. Combination of all of these factors may introduce error into further calculation of total current. For this reason, it is hypothesized that a deviation of ± 10% will account for the rough estimate of the above-calculated values. So, for cortisone, the diffusion coefficient range is 2.58*10^{-10} - 3.16*10^{-10} m^2/s. For cortisol, the same range is 2.56*10^{-10} - 3.12*10^{-10} m^2/s.

Finally, estimating the diffusion coefficients eliminates two variables from the list of unknowns. The following section explains the calculation of dimensionless current (summation term of equation 3.26).

4.2 Calculation of Peak Dimensionless Current

The dimensionless current is calculated using the system of equations 3.19 through 3.24 from chapter 3. First, Square Wave Voltammetry (SWV) excitation voltage is calculated using equation 3.19 over so many half cycles.

$$E_m = E_i - \left[Int\left(\frac{m+1}{2}\right) - 1 \right] \Delta E_s + (-1)^m \Delta E_p \quad (for\ m \geq 1) \tag{3.19}$$

All the parameters from this equation are known (E_i = 0.08V, ΔE_s = 0.004V, ΔE_p = 0.02V, f = 8Hz) [15], so modeling the waveform presents a simple task (see figure 4.2).

Next, the value of E_m (from equation 3.19) is used in conjunction with $E_{1/2}$ (which is calculated to be approximately 0.039V**,** since $E^{0'}$ was found to be 0.04V [14]) to determine the balance between concentrations of oxidative and reductive species at the working electrode by equation 3.20.

$$\theta_m = \frac{C_O(0,t)}{C_R(0,t)} = \exp\left[\frac{nF}{RT}(E_m - E_{1/2}) \right] \tag{3.20}$$

This balance changes every half cycle and is used further down in the estimation of dimensionless peak current. Equations 3.20 and 3.22 are then combined into equation 3.21 to find the next term in a sequence, *Q*.

$$\xi = \left(\frac{D_O}{D_R} \right)^{0.5} \tag{3.22}$$

$$Q_i = \frac{\xi\theta_i}{1+\xi\theta_i} \quad (i>0) \quad Q_0 = 1 \tag{3.21}$$

Finally, equation 3.23 yields the dimensionless current at any particular instance, while equation 3.24 represents the total net current (or the difference between the forward and reverse dimensionless currents) – analogous to equation 3.15. The peak dimensionless current is obtained from equation 3.24, and is the highest point in the curve - $\Delta\psi_p$ (see figure 4.3). It is determined to equal 0.4247.

$$\psi_m = \sum_{i=1}^{m} \frac{Q_{i-1} - Q_i}{(m-i+1)^{0.5}} \tag{3.23}$$

$$\Delta\psi_m = \psi_m - \psi_{m+1} \tag{3.24}$$

Using the frequency of 8Hz for the square wave excitation [15], it is calculated that the period of the square wave is 0.125s (an inverse of frequency). It then follows that the half cycle of the square wave lasts 0.0625s. Using the logic that current is probed every 0.0625s (first in forward then in reverse direction), it is hypothesized that the whole measurement can be performed in the amount of time it takes the square wave excitation to reach a certain level lower than that of $E_{1/2}$. In other words, forward and reverse currents become similar and electrolysis starts to occur at the diffusion controlled rate. In this case, it is hypothesized that the whole measurement could be performed in 5 seconds (see figure 4.4). It is assumed that estimating the diffusion coefficient to 10% does not affect the results since the error is canceled by the equation 3.22. In other words, the term ξ will not change if the diffusion coefficient is 10% larger (or smaller), since the ratio remains the same.

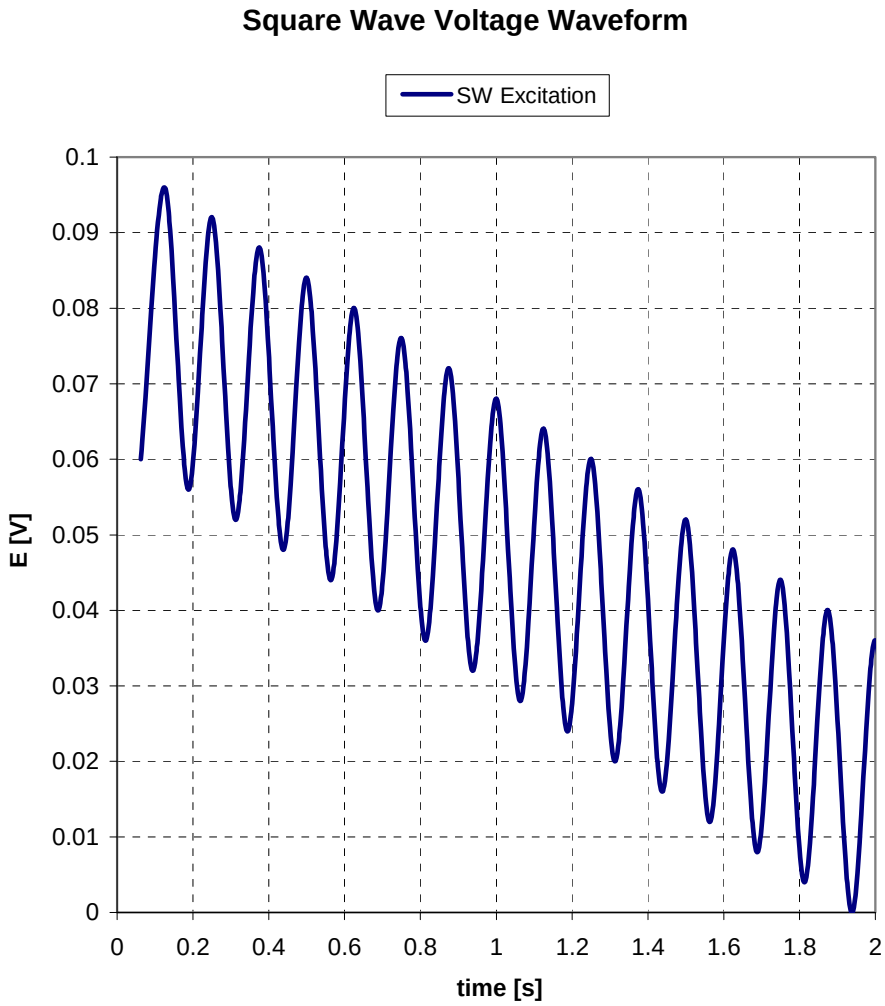

Figure 4.2: Simulation of SW Excitation on Working Electrode

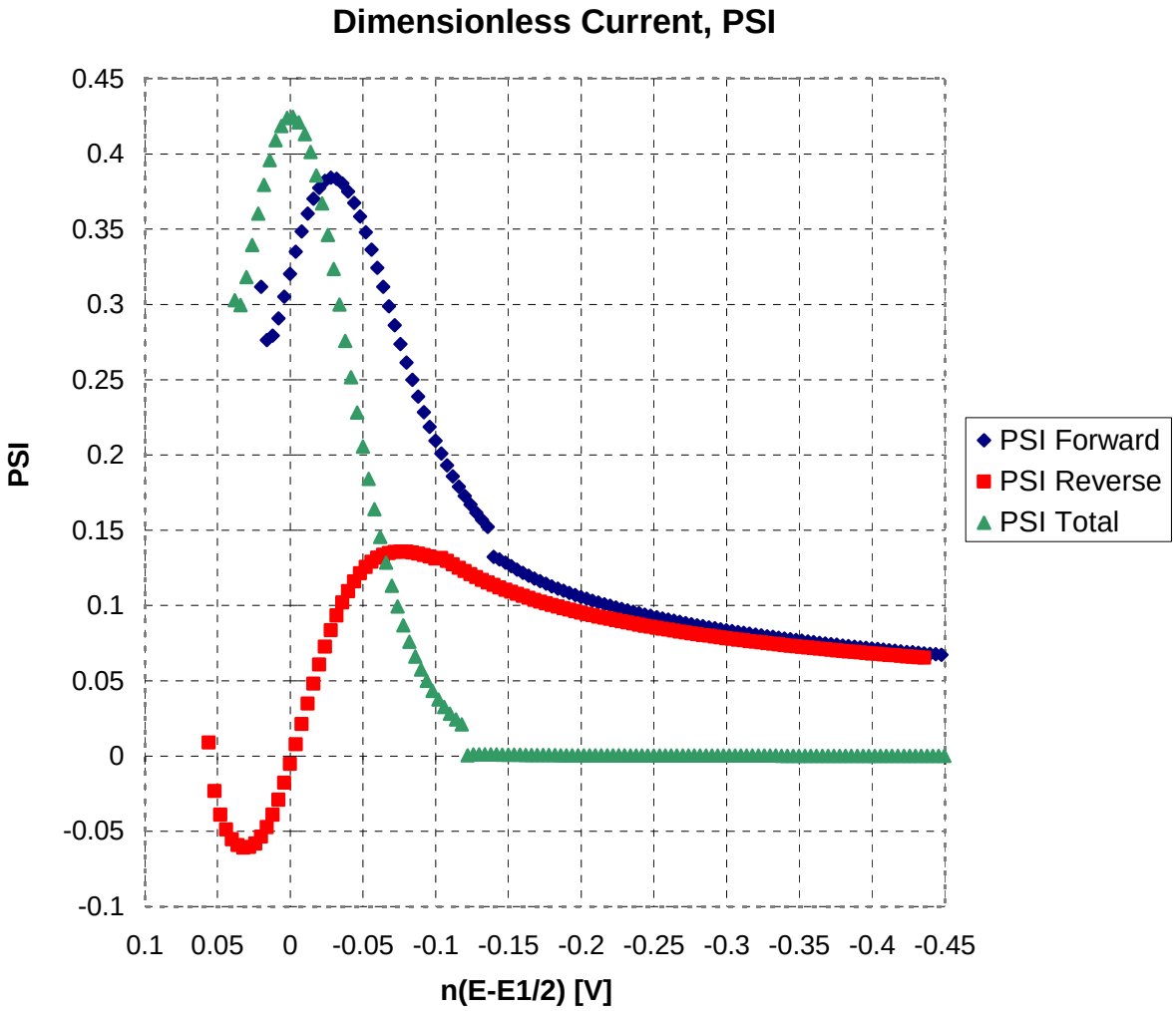

Figure 4.3: Simulation of Dimensionless Current

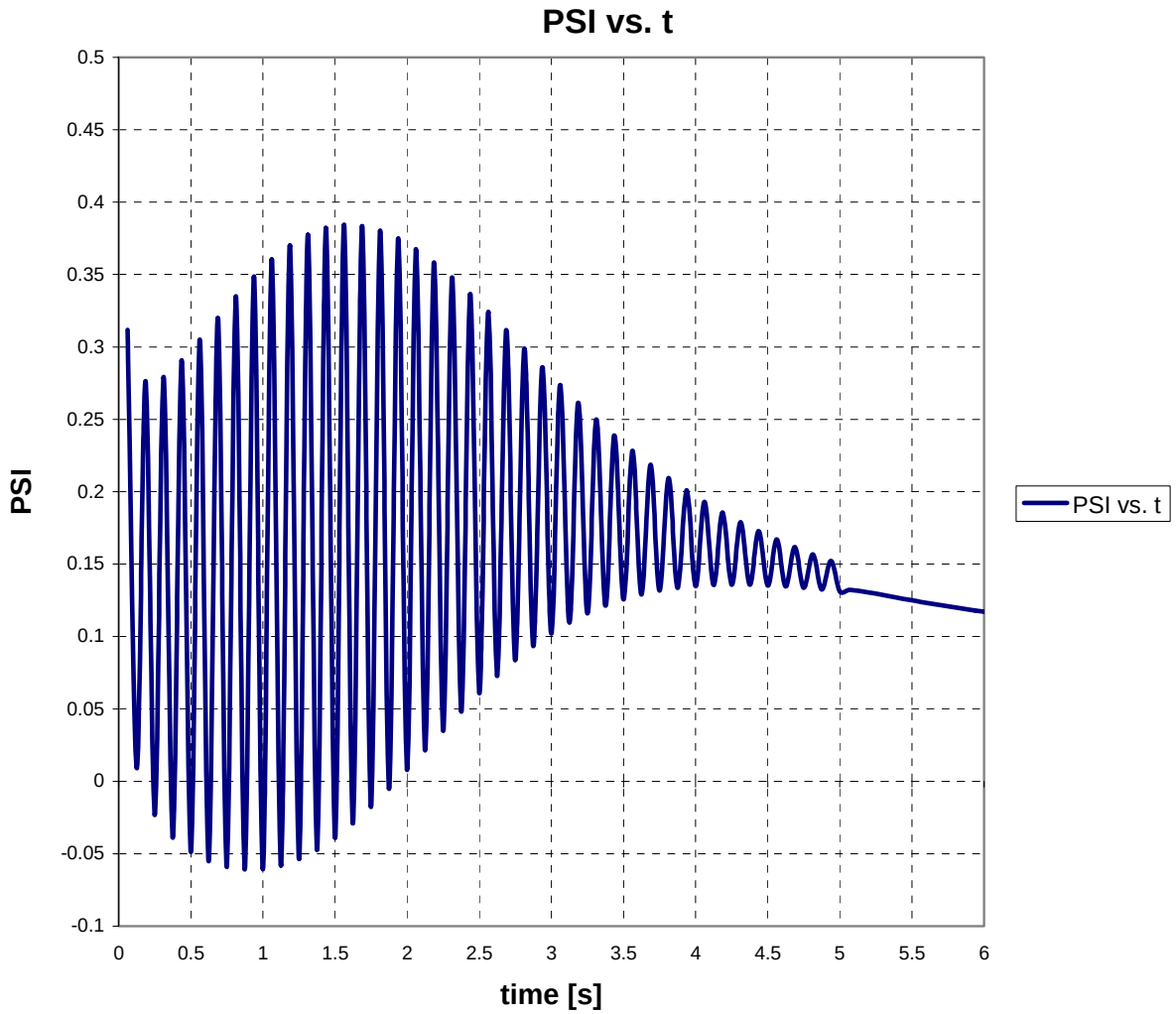

Figure 4.4: Simulation of Dimensionless Current Over Time

4.3 Calculation of Surface Area of Working Electrode

After estimating the dimensionless current, the surface area of the working electrode remains the last unknown in equation 3.26. However, in order to estimate the surface area of the electrode, it is first necessary to estimate the peak currents obtained in the lab experimentally (from figures 2.7a and 2.7b). These peak currents are necessary because the area is estimated from equation 4.1, which is a modified form of equation 3.25.

$$A = \frac{\pi^{0.5} t_p^{0.5} \Delta i_p}{\Delta\psi_p n F D_O^{0.5} C_O^*} \qquad 4.1$$

Dimensionless peak current value determined in the previous section ($\Delta\psi_p$ = 0.4247) is used in the above equation. The value extrapolated from table 3.1 ($\Delta\psi_p$ = 0.4647) can also be used; however, square wave voltammogram could not be obtained since this value strictly represents a single value at the peak. In other words, it would not yield a continuous line which illustrates the potential at which peaks occur. But to verify the information, both methods will be performed and compared for consistency.

Finally, looking at the figures 2.7a and 2.7b, eight different current peaks are estimated for each concentration of hormone added to the cell. An important thing to note is that the concentrations must be converted to appropriate units. A good check would be to write out the unit equation using equation 4.1, and to determine whether the final result is m^2, such as performed in section 4.1.

$$\frac{\pi^{0.5} t_p^{0.5} \Delta i_p}{\Delta\psi_p n F D_O^{0.5} C_O^*} = \frac{\left[\sqrt{s}\right] * [A]}{\left[\frac{C}{mol}\right] * \left[\sqrt{\frac{m^2}{s}}\right] * \left[\frac{mol}{m^3}\right]} = \frac{\left[\sqrt{s}\right] * \left[\frac{C}{s}\right]}{\left[\frac{C}{mol}\right] * \left[\sqrt{\frac{m^2}{s}}\right] * \left[\frac{mol}{m^3}\right]} = [m^2]$$

Table 4.1: Calculation of Surface Area Using Dimensionless Peak Current From Figure 4.3

Concentration [mol/m^3]	**Peak Current [A] (fig. 2.7a and 2.7b)**	**Diffusion Coefficient [m^2/s]**	**Net PSI (fig. 4.3)**	**Surface Area [m^2]**
0.01	8.01E-06	2.87E-10	0.4247	5.11E-04
0.02	1.68E-05	2.87E-10	0.4247	5.36E-04
0.03	2.87E-05	2.87E-10	0.4247	6.10E-04
0.04	4.41E-05	2.87E-10	0.4247	7.04E-04
0.05	6.45E-05	2.87E-10	0.4247	8.23E-04
0.06	9.35E-05	2.87E-10	0.4247	9.94E-04
0.07	1.27E-05	2.87E-10	0.4247	1.16E-04
0.08	1.55E-05	2.87E-10	0.4247	1.24E-04

After estimating the areas by using the peak value from the dimensionless graph, a second method of estimating the area is performed. The dimensionless peak current value ($\Delta\psi_p = 0.4647$) from table 3.1 is used based on the square wave excitation parameters specified. This is a faster, simpler method since it does not involve software analysis.

Table 4.2: Calculation of Surface Area Using Dimensionless Peak Current From Table 3.1

Concentration [mol/m^3]	**Peak Current [A] (fig. 2.7a and 2.7b)**	**Diffusion Coefficient [m^2/s]**	**Net PSI (Table 3.1)**	**Surface Area [m^2]**
0.01	8.01E-06	2.87E-10	0.4647	4.67E-04
0.02	1.68E-05	2.87E-10	0.4647	4.90E-04
0.03	2.87E-05	2.87E-10	0.4647	5.58E-04
0.04	4.41E-05	2.87E-10	0.4647	6.43E-04
0.05	6.45E-05	2.87E-10	0.4647	7.52E-04
0.06	9.35E-05	2.87E-10	0.4647	9.09E-04
0.07	1.27E-05	2.87E-10	0.4647	1.05E-04
0.08	1.55E-05	2.87E-10	0.4647	1.13E-04

It is evident from the above calculations that the surface areas using different values of the dimensionless peak current vary roughly up to 10%. During the final current estimate, it is important to keep the above calculations separate. They may be describing the same entities, but the methods utilized to calculate that entity are different.

Also, looking at the above values for the surface area of the nanowires, it might seem surprising that such small particles could create such a large surface area of the working electrode. In order to understand this better, it is imperative to refer back and analyze the original method utilized to fabricate the *Au* nanowires [15]. Understanding the amount of surface area that the entire set of nanowires from the Whatman disc can form determines whether the above surface area calculations make sense.

The nanowires were fabricated by electroplating in Techni Gold 25 ES solution for 1 hour [15]. Graphical representation of the Whatman disc clarifies physical dimensions of the *Au* nanowires (see figure 4.5).

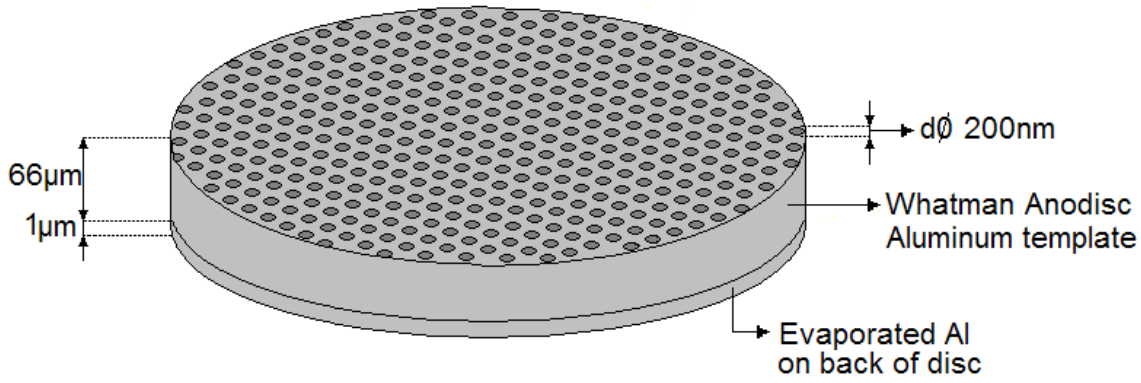

Figure 4.5: Graphical Representation of Whatman Disc

Electroplating for 1 hour creates a nanowire that is roughly 20µm in length. However, after releasing the nanowires in KOH and then methanol, it is hypothesized

that they break in half since they are thought to be extremely brittle. Also, for the sake of calculation, it is assumed that the nanowires are perfectly cylindrical. Taking this into account (perfect cylinder; 10μm in length; 200nm base diameter) the surface area of a single nanowire is calculated to be $6.35*10^{-12}$ m^2.

The Whatman disc comes in two sizes, 13mm and 26mm in diameter. Also, the pore density ranges between 10^{13}-10^{14} holes per meter squared [31, 36]. Depending on which size of the disc is selected, the total number of holes per disc is $2.65*10^{9}$ (for the 13mm diameter disc) and $1.06*10^{10}$ (for 26mm diameter disc). Multiplying these numbers by the surface area of a single nanowire yields a total surface area of $1.68*10^{-2}$ m^2 ($168cm^2$) for a 13mm diameter disc and $6.74*10^{-2}$ m^2 ($674cm^2$) for a 26mm diameter disc.

Finally, the surface areas from all the nanowires in the disc are compared with the surface areas of the working electrode thought to be present in the cell. It is obvious that the total surface area of the nanowires thought to be in the cell makes only a small fraction of the total surface area produced by all the nanowires that are in either size Whatman disc. Therefore the nanowires do indeed have the potential for creating a total surface area comparable to that determined independently from the electrochemical calculations shown earlier in tables 4.1 and 4.2.

4.4 Calculation of Total Peak Current for an Electrochemical Response

After all the unknown parameters have been estimated, the total peak current of the electrochemical system can finally be calculated and graphed using equations 3.25 and 3.26

$$\Delta i_p = \frac{nFAD_O^{0.5} C_O^*}{\pi^{0.5} t_p^{0.5}} \Delta\psi_p \qquad 3.25$$

$$i_m = \frac{nFAD_O^{0.5} C_O^*}{\pi^{0.5} t_p^{0.5}} \sum_{i=1}^{m} \frac{Q_{i-1} - Q_i}{(m-i+1)^{0.5}} \qquad 3.26$$

Equation 3.25 utilizes the second part of area calculations (table 4.2) illustrated in the previous section. This equation yields single point current peaks at a particular concentration. These values are compared against figure 2.8 from experimental analysis.

Equation 3.26 illustrates the entire square wave voltammogram and highlights the half potential of the cell (since that is the point where peak occurs). The first part of the equation ($\frac{nFAD_O^{0.5} C_O^*}{\pi^{0.5} t_p^{0.5}}$) represents a constant that is combined with the graph of the dimensionless net current ($\sum_{i=1}^{m} \frac{Q_{i-1} - Q_i}{(m-i+1)^{0.5}}$) from figure 4.3. The areas from table 4.1 (section 4.3) are incorporated into this equation. The values are also compared against the ones obtained in figure 2.8 from experimental analysis.

Further, like in previous sections, it is recommended to write out the equation with units to make sure errors do not carry over (the final result is in Ampere). In order to do this, all the parameters and their respective values and units are listed below.

1. n – Number of electrons involved in reaction = 1 (when cortisone is converted to cortisol it releases 1 electron)
2. F – Faraday constant $\cong$ 96,500 C mol^{-1}
3. A – surface area of working electrode – see section 4.3 (steps 1-8)

4. D_O – Diffusion coefficient for O-species $\cong 2.87*10^{-10}$ m^2/s

5. C_O^* - Bulk concentration of O-species = 10-80μM (figures 2.7a and 2.7b) or 0.01-0.08 mol/m^3

6. t_p – half-cycle of the square wave = 0.0625 seconds

7. $\Delta\psi_p$ – estimated from figure 4.3 $\cong$ 0.4247

$$\frac{nFAD_O^{0.5}C_O^*}{\pi^{0.5}t_p^{0.5}} = \frac{\left[\frac{C}{mol}\right]*\left[m^2\right]*\left[\sqrt{\frac{m^2}{s}}\right]*\left[\frac{mol}{m^3}\right]}{\sqrt{s}} = \left[\frac{C}{\sqrt{s}*\sqrt{s}}\right] = \left[\frac{C}{s}\right] = [A]$$

After performing a unit check, theoretical current peaks are finally graphed and calculated using Microsoft Excel. The maximum value of each peak is then determined and graphed against each concentration. The theoretical current peaks are compared against experimental current peaks from chapter 2 (see figures 4.6 and 4.7). Error bars are set to 10% to account for hypothesized percent error when estimating the diffusion coefficient.

Equation 3.25 is used in order to see whether the results would match if the value of dimensionless peak current from table 3.1 were used. So the only two parameters that changed from the list above are the surface area calculations (step 3) and dimensionless peak current (step 7). In this instance, surface area equation 4.1 would utilize calculations from table 4.2 (section 4.3), while dimensionless peak current would equal 0.4647. Likewise, error bars are set to 10%. The results are discussed in chapter 5.

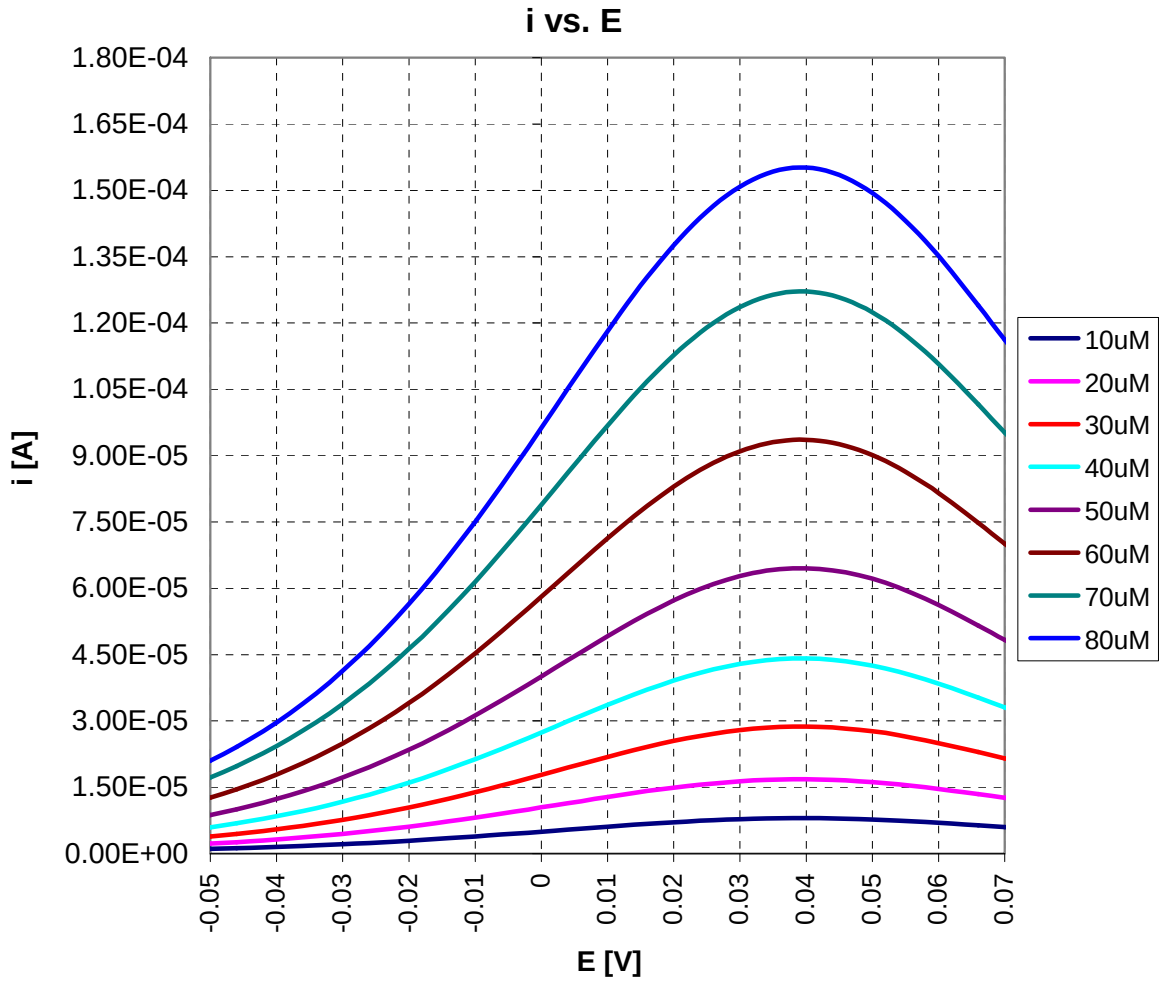

Figure 4.6: Theoretically Calculated SW Voltammogram for Different Concentrations of Cortisone/Cortisol

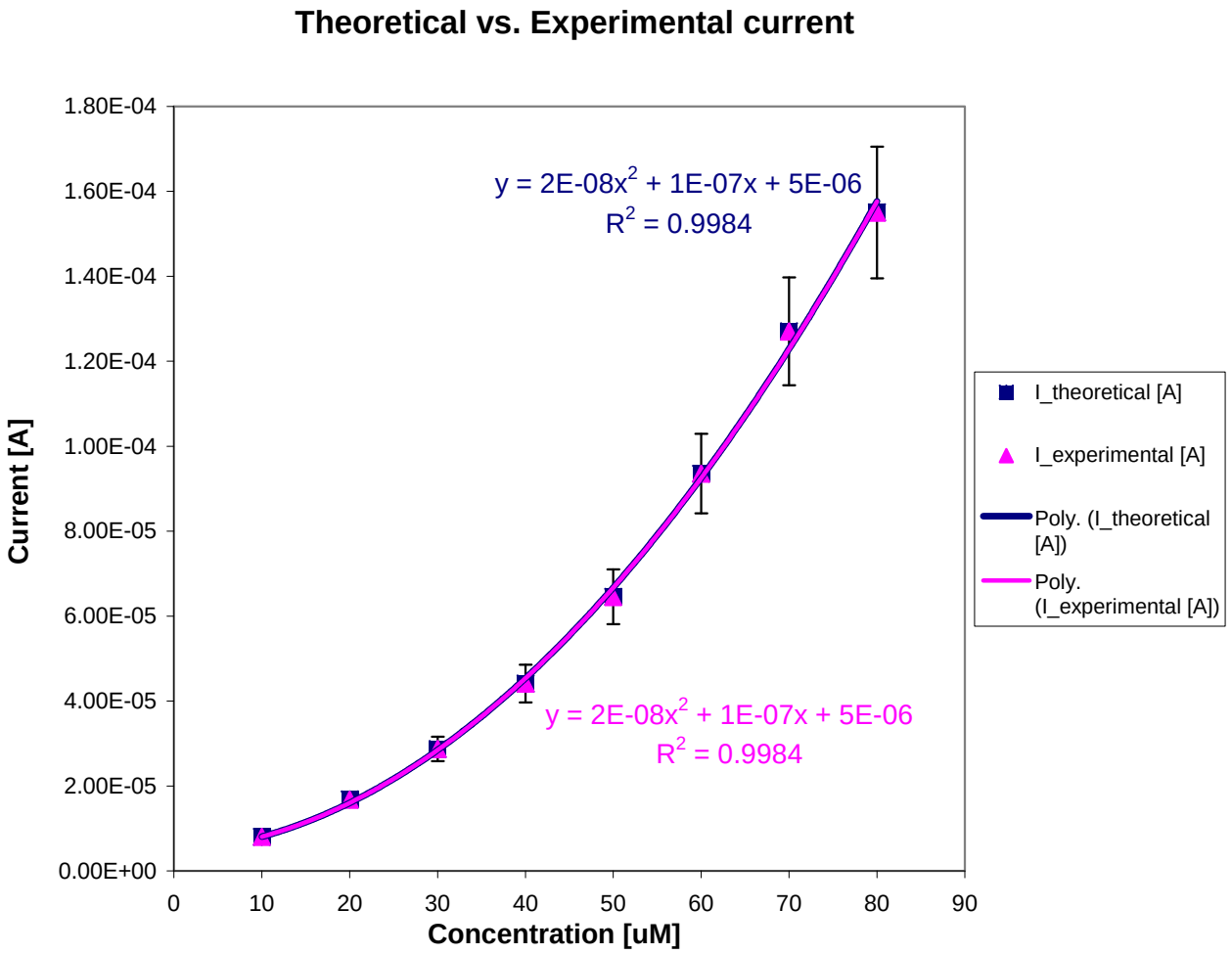

Figure 4.7: Theoretically Calculated Current Based on Different Concentrations of Cortisone/Cortisol Using Dimensionless Peak Current From Figure 4.3

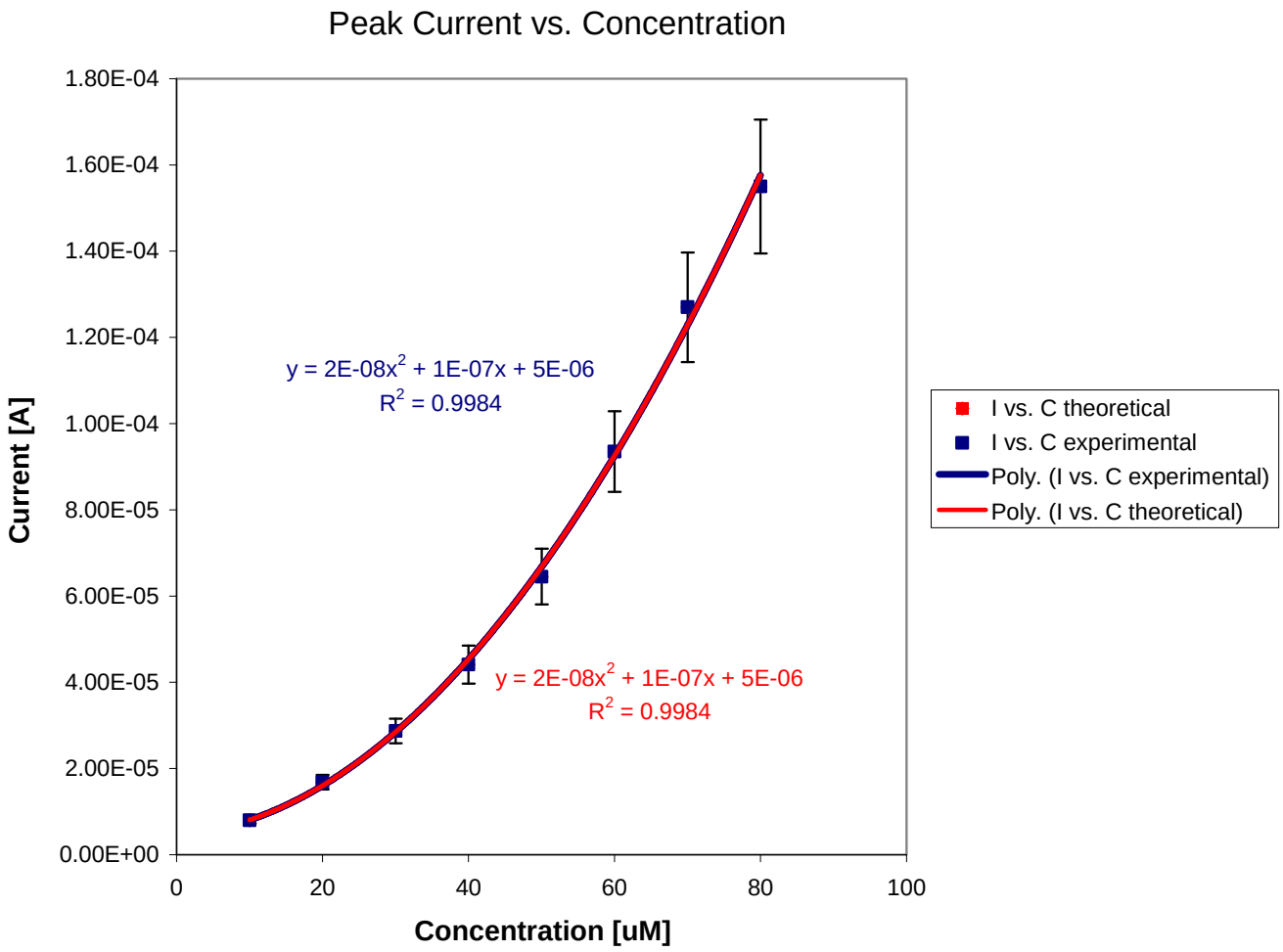

Figure 4.8: Theoretically Calculated Current Based on Different Concentrations of Cortisone/Cortisol Using Dimensionless Peak Current From Table 3.1

CHAPTER 5

DISCUSSION AND FUTURE WORK

In this research, a theoretical model has been developed for a sensor to detect the cortisol hormone. An in-depth look into Square Wave Voltammetry resulted in the information needed to optimize the design of the sensor itself. The following conclusions are primarily based on numerical analysis of the data. At the end of this chapter, suggestions to optimize the design of the sensor are given.

5.1 Discussion

The greatest challenge of this analysis was to estimate the surface area of the working electrode to aid in the approximation of the current during the electrochemical measurement. The theoretically estimated values from figures 4.7 and 4.8 are mirror images of the experimental values shown in figure 2.8 (unsurprisingly, because figures 4.7 and 4.8 are after all reverse-engineered by using the values from figure 2.8). However, one fundamental question arises from the entire analysis that deals with the accuracy and reliability of the surface area of the working electrode (estimated in section 4.3) that is used to estimate curves in figures 4.7 and 4.8. Are the values calculated in table 4.1 (section 4.3) more precise than values calculated in table 4.2 (section 4.3), even though they fall within 10% tolerance of one another? To better answer this question, it

is necessary to refer to the original process utilized to align the nanowires as the working electrode of the sensor.

Alignment of *Au* nanowires was completed utilizing the dielectrophoresis technique discussed in chapter 3. First, the resistance was checked between electrodes to ensure complete isolation between the positive and negative microelectrode using a simple Digital multi-meter. 200µl of nanowire-methanol solution was then dispersed over the microelectrodes using a syringe. Agilent 33250 waveform generator was connected to microelectrodes and programmed to output 10 V_{RMS} at 1kHz. This signal was applied over the period of 15 seconds. After this initial period, the excess nanowire solution was removed, and the working area was washed with pure methanol. Potential and frequency were then varied gradually over time up to $50V_{RMS}$ and 10kHz for an additional 30 seconds. The assembly was observed by monitoring the voltage drop over the series 1kΩ resistor and was later verified with a scanning electron microscope (SEM). The set-up was left at room temperature overnight to dry off. Finally, resistance was checked again between microelectrodes to ensure the presence of nanowires which indicated alignment. Resistance should decrease during the second check, suggesting a short path between the electrodes.

The problem with the above method is that the amount of nanowires dispersed with 200µl of methanol cannot be controlled. If the process is required to be repeated multiple times, the sole number of nanowires becomes unpredictable and starts to vary, making the surface area parameter from equation 3.26 a variable. Further manipulation of the working area of the sensor (like washing the area with piranha solution, which is done to activate the *Au* nanowires and attach cortisol antibodies) may remove the loose

nanowires off the sensor completely. This is a factor that only adds variability to the design.

But even if the above-stated problems were not an issue, the dielectrophoretic alignment of the nanowires presents another challenge. The force of the electric field during the alignment will not align the nanowires to perfectly bridge the gap between electrodes. The final outcome is more similar to a random, uncontrolled alignment as shown in figure 5.1. Some nanowires may get welded to the microelectrodes under the influence of electric field; others may just stay in contact with the microelectrodes without forming a firm joint, while some nanowires may not be in contact with the microelectrodes at all. The latter presents a problem because the excitation voltage never reaches this portion of the working electrode, thus skewing the result.

The above factors result in the surface area parameter being a variable, which makes it (and the sensor) extremely difficult to study. In order to overcome this problem, it is necessary to design a sensor with a fixed electrode surface area. For example, evaporating a fixed amount of *Au* onto a *Si* chip and creating an electrochemical cell around it.

On the other hand, utilizing the nanowires brings some advantages. The surface area provided by a small fraction of the nanowires is comparable to the surface area of evaporating a larger amount of *Au* onto a wafer. For a large scale operation, evaporating the *Au* onto a *Si* wafer uses more *Au*; thus raising the cost. Creating a larger surface area on multiple wafers by using nanowires from a single Whatman disc can lower the cost substantially. Also, because of their size, nanowires can potentially achieve higher sensitivity, even though the area footprint is significantly reduced.

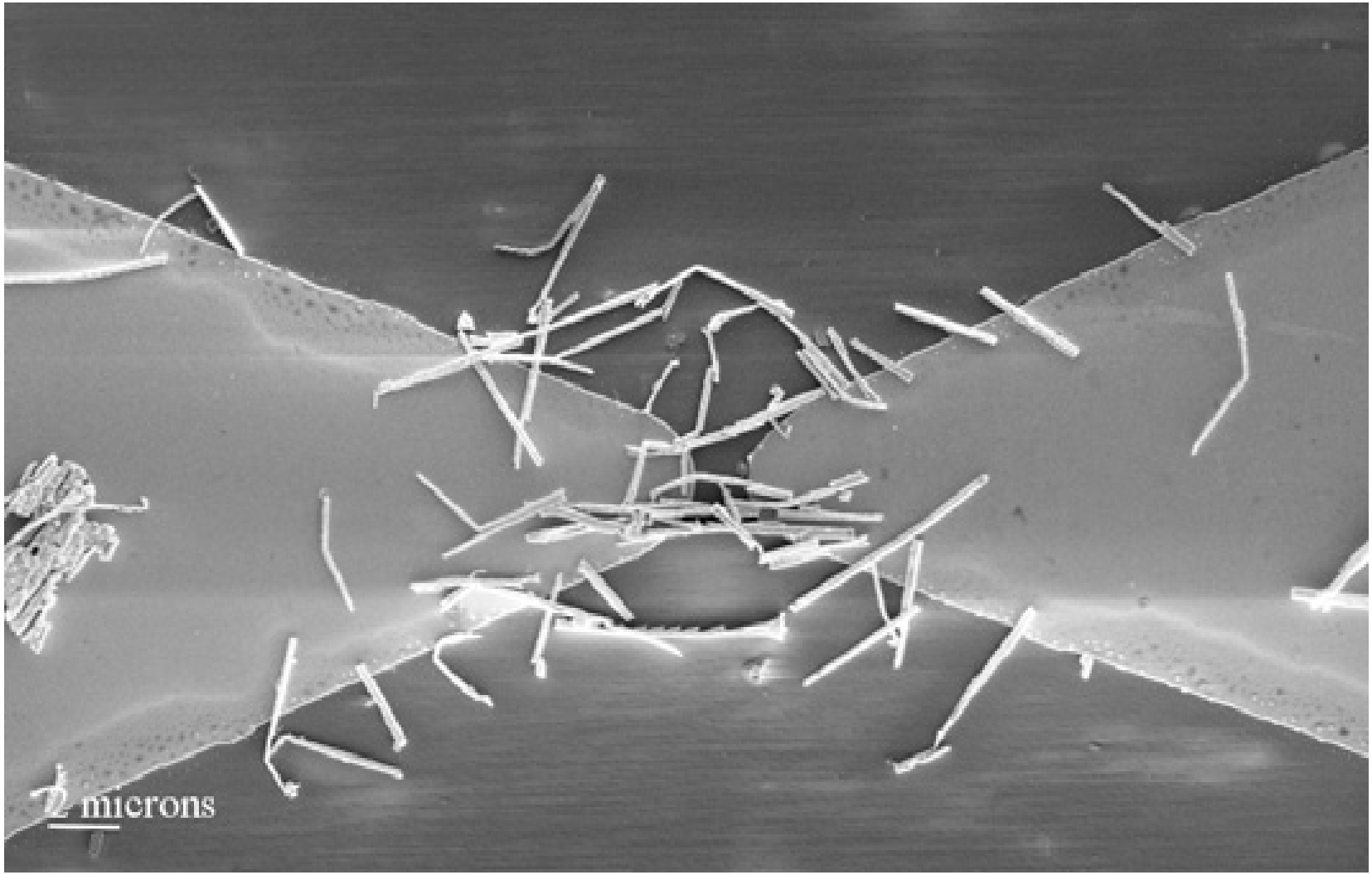

Figure 5.1: Random Alignment of Nanowires. Reprinted from Nanotechnology, 16, Boote et al., Dielectrophoretic manipulation and electrical characterization of gold nanowires, 1500-1505, Copyright (2005), with permissions from IOP Publishing Ltd. and S.D. Evans.

The reference electrode used for this sensor is fabricated externally and is suspended above the cell [14], making it another potential candidate for a variable since the electrode is inserted arbitrarily into the cell. This may introduce variations if the process is required to be repeated multiple times, since the location of the electrode is different every time.

Another problem with the external reference electrode is that there is a risk of shorting the surface of the metal between the reference electrode (which is freely suspended over the sensor in electrolyte) and the working and counter electrodes. It was observed in a separate unrelated experiment that shorting the reference electrode to the working and counter electrodes raises the temperature of PBS to a boiling point; thus making the test sample useless. Further MEMS analysis is necessary to come up with a design where all three electrodes (primarily the reference electrode) would be fixed in a cell. An example of such an electrode is illustrated in figure 5.2.

First, 300Å of *Ti* and *Ni* are evaporated (or sputtered) on the surface of the *Si* wafer. This step provides a good adhesion layer for the material that follows. Then, 5000Å of *Ag* is evaporated to create the first layer of the electrode. The epoxy is applied to the wafer to form the groove for bonding and the *AgCl* paste. Finally, the *AgCl* paste is added and the reference electrode characterization can be performed.

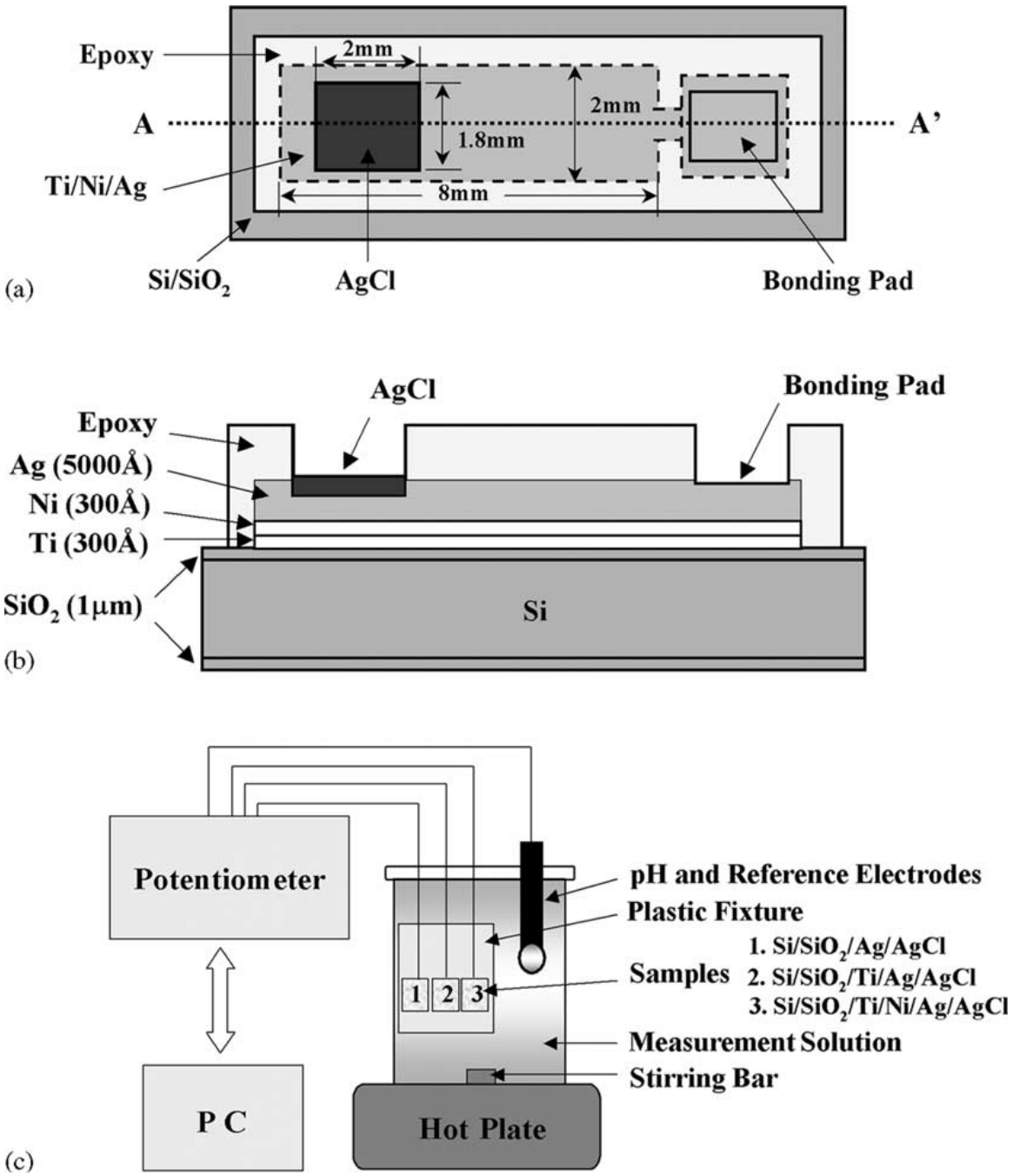

Figure 5.2: Ag/AgCl Reference Electrode. Reprinted from Sensors and Actuators B, 97, Kim et al., Enhancement of physical and chemical properties of thin film Ag/AgCl reference electrode using a Ni buffer layer, 348-354, Copyright (2004), with permission from Elsevier

Finally, having an open, unsealed cell where electrochemical measurements are performed leaves room for environmental interference with the set-up. Primarily, there is a human factor. Depending on the time of day the tests are performed (cortisol secretion is most active in the morning, least active at night) it may be possible to skew the results if the person performing the experiment disturbs the cell by being in close contact with it. More people in a surrounding area only increase the chance for an error. For this reason, there is a definite need for a sealed electrochemical cell as well as protective gear worn by the operator(s) performing the experiment.

5.2 Future Work

Based on the above observations, a recommendation is made for an improved design of an electrochemical sensor. First, for the time being, the nanowires are completely eliminated from the sensor since they introduce a problem when estimating the surface area of the electrode. Instead, *Au* is evaporated directly on the *Si* wafer to form the layer of the working electrode of a fixed surface area. Afterwards, the reference electrode is fabricated via the procedure described in the previous section; and the counter electrode is fabricated by evaporating a layer of *Pt* onto the surface of *Si* wafer. Finally, after activation and characterization of *Au*, the assay procedure can be performed (see figure 5.3). The measurement is recommended to be performed later in the day by an operator wearing all necessary protection to minimize interaction with the cell. The mathematical model developed in this thesis can be used to model the response of the sensor. After developing a repeatable model of the sensor, research to find a better alignment method of the nanowires is recommended to repeat the above experiment.

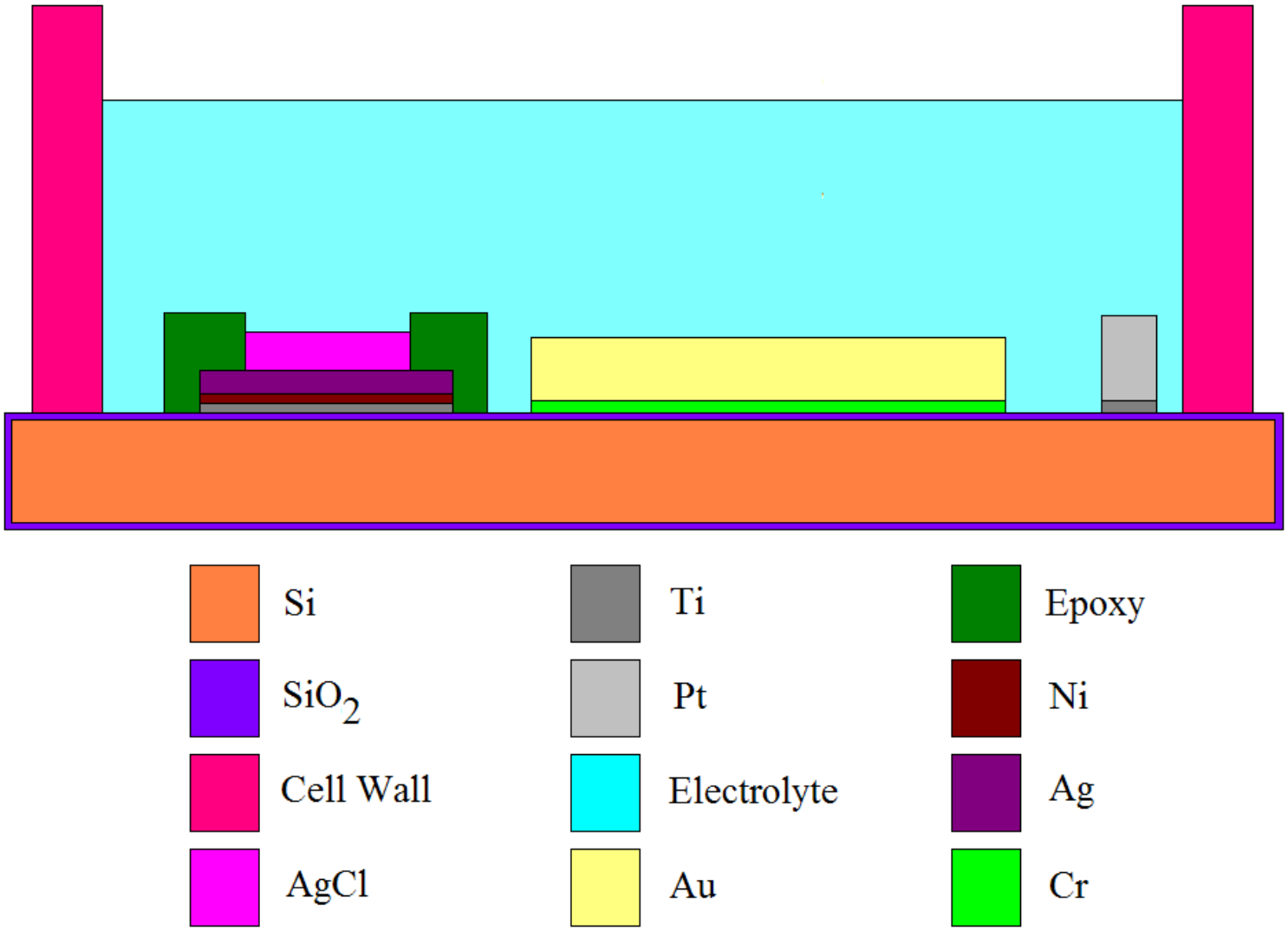

Figure 5.3: Graphical Representation of Design Improvement for BioMEMS El-Chem Sensor

REFERENCES

[1] Atkins P.W. *"Physical Chemistry"*. Oxford University Press. 1978.

[2] Bagotzky V.S. "*Fundamentals of Electrochemistry*". Plenum Press. 1993.

[3] Bard A.J. & Faulkner L.R. "*Electrochemical methods Fundamentals and Applications*". John Wiley & Sons, Inc. 2001. 2nd Edition.

[4] Bauer J.D., Ackerman P.G., & Toro G. "*Clinical Laboratory Methods*". The C.V. Mosby Company. 1974. 8th Edition.

[5] Boote J.J. & Evans S.D. 2005. "Dielectrophoretic manipulation and electrical characterization of gold nanowires". *Journal of Nanotechnology. Vol: 16: 1500-1505.*

[6] Castellano E.E., Main P., & Westbrook E. 1980. "The Disordered Structure of Cortisol (11β,17α,21-Trihydroxy-4-pregnene-3,20-dione) and Iodocortisol (11β, l 7β-Dihydroxy-2 l-iodo-4-pregnene-3,20-dione)." *Acta Crystallographica Section B. 36. Vol: 12: 3063-3067.*

[7] Citizendium. Online encyclopedia. 10/09/2008 [http://en.citizendium.org/wiki/Cortisol]

[8] Flodmark L.E.W., Urke H.A., Halleraker J.H., Arnekleiv J.V., Volestad L.A., & Poleo A.B.S. 2005. "Cortisol and glucose responses in juvenile brown trout subjected to a fluctuating flow regime in an artificial stream". *Journal of Fish Biology. Vol: 60(1): 238–248.*

[9] Galimberti C.A., Magri F., Copello F., Arbasino C., Cravello L., Casu M., Patrone V., & Murialdo G. 2005. "Seizure Frequency and Cortisol and Dehydroepiandrosterone Sulfate (DHEAS) Levels in Women with Epilepsy Receiving Antiepileptic Drug Treatment". *Epilepsia. Vol: 46(4): 517–523.*

[10] Goulding N.J. & Flower R.J. (Editors). *"Glucocorticoids (Milestones in Drug Therapy)".* Birkhauser. 2001. 1st Edition.

[11] Henry J.B. "*Clinical Diagnosis and Management by Laboratory Methods*". W.B. Saunders Company. 1997. 19th Edition.

[12] Jones C. "*The Adrenal Cortex*". Cambridge University Press, 1957.

[13] Kissinger P.T. & Heneman W.R. "*Laboratory Techniques in Electroanalytical Chemistry*". Marcel Dekker, Inc. 1996. 2nd Edition.

[14] Kumar A., Ph.D. Personal Interview. University of South Florida. 04/08/2008.

[15] Kumar A., Aravamudhan S., Gordic M., Bhansali S., & Mohapatra S.S. 2007. "Ultrasensitive detection of cortisol with enzyme fragment complementation technology using functionalized nanowires." *Biosensors and Bioelectronics*. *Vol: 22: 2138-2144.*

[16] Larkin K.T., Semenchuk E.M., Frazer N.L., Suchday S., & Taylor R.L. 1998. "Cardiovascular and behavioral response to social confrontation: measuring real-life stress in the laboratory". *Annals of Behavioral Medicine. Vol: 20(4): 294-301*.

[17] Lin C.L., Wu T.J., Machacek D.A., Jiang N.S., & Kao P.C. 1997. "Urinary Free Cortisol and Cortisone Determined by High Performance Liquid Chromatography in the Diagnosis of Cushing's Syndrome". *Journal of Clinical Endocrinology and Metabolism. Vol: 82(1): 151-155*.

[18] Marieb E.N. "*Human Anatomy and Physiology*". Pearson Benjamin Cummings. 2004. 2nd Edition.

[19] Martin C.R. "*Endocrine Physiology*". Oxford University Press. 1985.

[20] Monk P.M.S. "*Fundamentals of Electroanalytical Chemistry*". John Wiley & Sons, Inc. 2001.

[21] Nomura S., Fujitaka M., Jinno K., Sakura N., & Ueda K. 1996. "Clinical significance of cortisone and cortisone/cortisol ratio in evaluating children with adrenal diseases". *Clinica Chimica Acta. Vol: 256(1): 1–11.*

[22] O'Dea J.J., Osteryoung J., & Osteryoung R.A. 1981. "Theory of Square Wave Voltammetry for Kinetic Systems". *Analytical Chemistry. Vol: 53(4): 695-701.*

[23] Petkus M.M., McLauchlin M., Vuppu A.K., Rios L., Garcia A.A., & Hayes M.A. 2006. "Detection of FITC-cortisol via Modulated Supraparticle Lighthouses". *Analytical Chemistry. Vol: 78: 1405–1411.*

[24] Pfaff D.W., Phillips I.M., & Rubin R.T. "*Principles of Hormone/Behavior Relations"*. Elsevier Academic Press. 2004.

[25] Pohl H.A. "*Dielectrophoresis*". Cambridge University Press. 1978

[26] Ramaley L. & Krause M.S. Jr. 1969. "Theory of Square Wave Voltammetry". *Analytical Chemistry. Vol: 41(11): 1362-1365.*

[27] Ramaley L. & Krause M.S. Jr. 1969. "Analytical Application of Square Wave Voltammetry". *Analytical Chemistry. Vol: 41(11): 1365-1369.*

[28] Rifkin S.C. & Evans D.H. 1976. "General Equation for Voltammetry with Step-Functional Potential Changes Applied to Differential Pulse Voltammetry". *Analytical Chemistry. Vol: 48(11): 1616-1618.*

[29] Shikii K., Sakamoto S., Seki H., Utsumi H., & Yamaguchi K. 2004. "Narcissistic aggregation of steroid compounds in diluted solution elucidated by CSI-MS, PFG NMR and X-ray analysis". *Tetrahedron. Vol: 60: 3487-3492.* Retrieved on 08-01-2008 from the *Cambridge Structural Database.*

[30] Stulik K. & Pacakova V. "*Electroanalytical measurements in flowing liquids*". Ellis Horwood Limited. 1987.

[31] Sun K., Ph.D. Candidate. Personal Interview. University of South Florida. 09/05/2008.

[32] Tepperman J. "*Metabolic and Endocrine Physiology*". Yearbook Medical Publishers. 1968. 2nd Edition.

[33] Turner J.A., Christie J.H., & Osteryoung R.A. 1977. "Square Wave Voltammetry at the Dropping Mercury Electrode: Theory". *Analytical Chemistry. Vol: 49(13): 1899-1903.*

[34] Turner J.A., Christie J.H., Vukovic M., & Osteryoung R.A. 1977. "Square Wave Voltammetry at the Dropping Mercury Electrode: Experimental". *Analytical Chemistry. Vol: 49(13): 1904-1908.*

[35] Vanysek P. "*Modern Techniques in Electroanalysis*". John Wiley & Sons. 1996.

[36] Whatman Inc. Technical Data. Anopore Inorganic Membranes. 09/05/2008. [http://www.whatman.com/PRODAnoporeInorganicMembranes.aspx]